

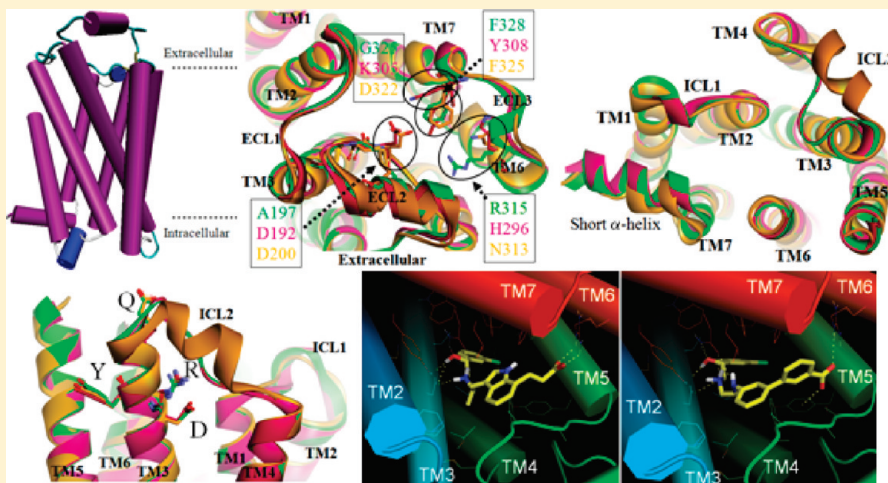
Structural Basis for the β -Adrenergic Receptor Subtype Selectivity of the Representative Agonists and Antagonists

Kuldeep K. Roy and Anil K. Saxena*

Division of Medicinal and Process Chemistry, Central Drug Research Institute, CSIR, Lucknow 226 001, India

Supporting Information

ABSTRACT:



The β_3 -adrenergic receptor (β_3 -AR) selectivity over β_1 - and β_2 -ARs has been the most important aspect for successful therapeutic agents for obesity and type-II diabetes, as the concomitant activation of β_1 - and β_2 -ARs would lead to undesirable side effects, such as increased heart rate. In order to explore the structural basis for the β -AR subtype selectivity of agonists and antagonists, a three-dimensional structure of until date unresolved β_3 -AR has been modeled, compared with the resolved X-ray structures of β_1 - and β_2 -ARs, and used to study its stereoselective binding with until-date known diverse classes of representative agonists and antagonist. The obtained binding structures and calculated prime molecular mechanics-generalized Born surface area (MM-GBSA) binding free energies consistently reveal that while the subtype selectivity is strongly governed by the residues present in the extracellular ends of TM3, TM5, TM6, TM7 helices and of the ECL2 domain, the binding affinity is governed by the conserved residues present in the deep pocket limiting the degree of conformational and rotational freedoms to the bound ligand. The study demonstrates that the key structural requirements for the β_3 -selectivity are: (i) a negatively ionizable group (NIG) for direct interaction with β_3 -specific residue R315^{6,58}, (ii) a linker (9–10 Å length) between the protonated amine and NIG, and (iii) a substituted aryl ring directly attached to the β -hydroxyl carbon. The new computational insights acquired in this study are expected to be valuable in structure-based rational design of high-affinity agonists and antagonists with pronounced β_3 -selectivity for successful therapeutic agents for type-II diabetes and obesity.

INTRODUCTION

Overweight and obesity are the two globally foremost causes of death as they increase the risk for a number of chronic diseases, including diabetes and cardiovascular diseases.¹ The β_3 -adrenergic receptor (β_3 -AR) is present on the surface of both white and brown adipocytes and plays a significant role in regulating lipolysis and thermogenesis in rodent and human adipocytes.² The β_3 -AR has now been recognized as an attractive target for discovery and development of β_3 -AR agonists as therapeutic candidates for obesity and type-II diabetes.^{2,3} Recent clinical reports suggest that selective activation of β_3 -AR induces a variety of pharmacological effects, such as an increase in lipolysis and thermogenesis and also

an improvement of insulin-mediated glucose uptake in rodent models.⁴ Moreover, several investigations have also suggested newer therapeutic applications of β_3 -AR agonists in the treatment of gastrointestinal and overactive bladder (OAB) syndromes.⁴ The β_3 -AR selectivity over β_1 - and β_2 -ARs has been required for successful therapeutics for obesity and type-II diabetes,³ as the concomitant activation of β_1 - and β_2 -ARs would lead to undesirable side effects, such as increased heart rate and/or muscle tremors.

Received: February 21, 2011

Published: May 02, 2011

The β_3 -AR, along with β_1 - and β_2 -ARs, belong to the G-protein coupled receptor (GPCR) superfamily characterized by the presence of seven transmembrane (TM) domains separated by alternating three intracellular (N-terminal) and three extracellular (C-terminus) loop regions. Most members of this superfamily share a common topology, a seven TM helix bundle, even though sequence conservation across the superfamily is minimal. Despite these similarities, individual GPCRs mediate unique combinations of signal-transduction activities by coupling with multiple G-protein subtypes as well as G-protein-independent signaling pathways and complex regulatory processes.⁵ Thus, it has been of interest to study the functions of these integral proteins and their interactions with ligands. Certainly, detailed atomic resolution structures of these integral proteins would contribute significantly to our understanding of their molecular interactions and function. However, being integral membrane proteins, it is a daunting task to obtain atomic resolution structures of GPCRs because of their expressions at low levels in native tissues and poor thermal stability, causing difficulty to obtain a large amount of GPCRs, necessary for the high-resolution structural characterization. Additionally, GPCR structural biology projects seem to require several years of work before a new crystal structure can be solved. Currently, a large amount of data is available from various biophysical, ligand binding, and site-directed mutagenesis experiments on GPCRs. In such a scenario, the generation of three-dimensional (3D) structures of until date unresolved GPCRs, using various in-silico techniques based on the resolved structures of GPCRs and various indirect structural evidence obtained from a variety of biophysical techniques, seems to be a quite useful approach for understanding the structure and the functions of GPCRs.

The plausibility of model development using homology modeling techniques depends on the quality of the sequence alignment and the structural template(s). The homology modeling approach can be complicated by the presence of alignment gaps and by structure gaps in the template that arise from the poor resolution of the template structure. When a template shares a high-sequence identity with the target, the inclusion of additional templates may not improve the accuracy of the resulting model, however when all available templates share relatively low-sequence identity with the target, concomitant use may provide more accurate model than the model obtained with any single template. Though the rhodopsin structure made a major breakthrough in our understanding of these important proteins, the indiscriminant use of this crystal structure as a general GPCR template has been cautioned because of limited sequence identity between rhodopsin and other GPCRs in TM and extracellular domains.^{6–10} Recently, it is reported that a rhodopsin-based homology model of human β_2 -AR failed to predict the correct ligand-binding pose of carazolol, an inverse-agonist of β_2 -AR.¹⁰ This may be due to the fact that there is only ~22% sequence identity between rhodopsin and β_2 -receptor in the TM domains. These facts reflect the inappropriateness of rhodopsin for the model development of the unresolved GPCRs. Therefore, the reported rhodopsin-based models for β -AR by Furse and Lybrand¹¹ and other GPCRs are quite speculative and hence must be used with cautions.

In the recent past, a high-resolution (2.4 Å) crystal structure of the human β_2 -AR bound to the partial inverse agonist carazolol has been discovered.¹² In addition, a nanobody stabilized active-state crystal structure of the β_2 -AR bound to a full agonist has also been reported very recently (year 2011), but unfortunately this

structure has been solved at a very poor resolution (3.5 Å).¹³ The poor resolution of this active-state structure reflects the unsuitability of its use as template for the homology modeling. Furthermore, comparison of the active and inactive state structures of β_2 -AR has revealed minor changes in the binding pocket after activation.¹³ These subtle changes are associated with an 11 Å outward movement of the cytoplasmic end of TM6 and rearrangements of TM5 and TM7.¹³ These facts, such as the observed subtle changes in the binding pocket upon activation of β_2 -AR, and the utmost preference of the high-resolution template structure for homology modeling forecast that the high-resolution (2.4 Å) crystal structure of the human β_2 -AR bound to the partial inverse agonist carazolol¹² is the most suitable template for homology modeling of β_3 -AR.

Only limited mutagenesis information is currently available on structure–function relationships of the β_3 -adrenergic receptor. Using a series of β_3 -AR mutants and β_3 -/ β_2 -ARs chimaeras, Guan et al.¹⁴ demonstrated that the TM5 is decisive for binding with β_3 -AR-selective agonist BRL37344 and that the third intracellular loop (ECL3) of the β_3 -AR is critical for coupling to G-proteins. Recent studies on the W64R mutant showed that the maximal cAMP accumulation was significantly reduced in response to various β_3 -AR agonists when compared to wild-type β_3 -AR.¹⁵ Recently, Gros et al.¹⁶ attempted site-directed mutagenesis of the human β_3 -AR in order to explore the TM residues involved in ligand binding and signal transduction. In their study, a set of three contiguous residues, valine, leucine, and alanine (VLA) present at positions 48–50 of TM1 of the human receptor but are absent in all known rodent sequences, were thought to be important for species specificity. The mutation of G53 in the TM1 of the human β_3 -AR with F53 present in β_2 -AR led to an unaltered pharmacological profile of the human β_3 -AR in terms of specificity and selectivity.¹⁶ Furthermore, the mutation of D117^{3,32} in the TM3 with leucine residue in the β_3 -AR led to the suppression of ligand binding and signal transduction, and thus suggesting it to be essential for ligand binding and activation. The replacement of N312^{6,56} the TM6 by an alanine residue led to alterations in the signal transduction pathway.¹⁶ Finally, Granneman et al.,¹⁷ using chimeric and mutant β_1 - and β_3 -ARs, showed that the TM7 is a major determinant of β_3 -AR-subtype selectivity of agonists and demonstrated that the determinants of selective phenethanolamines, catecholamines, and propranolol action are quite distinct.

In view of above and prime requisite of β_3 -AR selectivity over β_1 - and β_2 -ARs for the development of successful therapeutics for obesity and type-II diabetes, an attempt has been made to elucidate the structural basis for subtype selectivity of agonists and antagonist among the β -AR subtypes using detailed computational studies, including homology modeling, docking, molecular dynamics simulation, and binding free energy calculation. The insights gained in this study provide scope for the rational design of high-affinity agonists and antagonists with pronounced subtype selectivity among β -adrenergic receptors.

■ RESULTS AND DISCUSSION

Multiple Sequence Alignment and Comparison of β_1 , β_2 , and β_3 -ARs. The amino acid sequence alignment is of prime importance because the modeling entirely depends on the structural homology. From the multiple sequence alignment (Figure 1), the global sequence identity (the fraction of amino acids that are the same between a pair of sequences after an

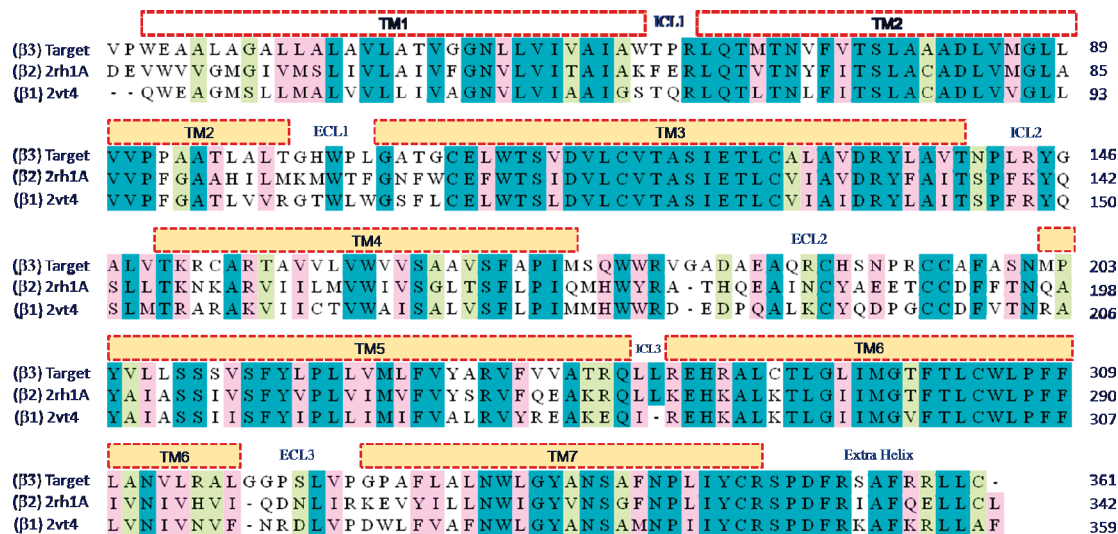


Figure 1. Multiple sequence alignment of turkey β_1 - (PDB ID: 2vt4), human β_2 - (PDB ID: 2rh1), and human β_3 -ARs (PAN = P13945). The seven TMs (TM1–TM7) are highlighted by an orange rectangle and are separated by extracellular (ECL1–3) and intracellular (ICL1–3) loops. The ICL3 residue is omitted here. The identical residues are shown in blue color, while residues with strong and weak similarity are shown in pink and greenish yellow colors.

Table 1. Comparison of Seven TMs of β_1 -, β_2 -, and β_3 -ARs in Terms of Corresponding Sequence Identity and Similarity

category	β_1 -, β_2 -, and β_3 -AR	β_1 - and β_3 -AR	β_2 - and β_3 -AR	β_1 - and β_2 -AR
	TM1	TM2	TM3	TM4
sequence identity (%)	36.7	46.7	46.7	56.7
	56.7	66.7	63.3	70.0
	70.6	76.5	73.5	82.4
	33.3	45.8	45.8	54.2
	45.5	48.5	57.6	69.7
	62.5	68.8	65.6	84.4
	50.0	70.8	62.5	50.0
sequence similarity (%)	50.0	53.3	60.0	73.3
	73.3	83.3	73.3	86.7
	88.2	91.2	88.2	94.1
	50.0	62.5	62.5	70.8
	66.7	66.7	75.8	90.9
	84.4	84.4	90.6	96.9
	75.0	87.5	75.0	79.2

alignment) and similarity (the score assigned based on an alignment using some similarity matrix) between the three subtypes of β -ARs have been found to be 48.0 and 66.5%, respectively, while the same have been between β_1 - and β_3 - (58.2 and 73.2%), β_2 - and β_3 - (55.7 and 72.5%), and β_1 - and β_2 -ARs (63.8 and 82.5%). The sequence identity and similarity between seven TMs of β_1 - and β_3 -ARs are 61.2 and 75.3% respectively, whereas between β_2 - and β_3 -ARs were 59.9 and 75.8% respectively. The sequence alignment of three subtypes of β -AR reveals that the third TM (TM3) was the most conserved domain with the highest consensus sequence identity and similarity of 70.6 and 88.2%, respectively (Table 1 and Figure 1), while the fourth TM (TM4) is the least conserved domain with sequence identity and similarity of 33.3 and 50.0%, respectively. The decreasing order of conservation among the

seven TMs of three subtypes of β -ARs is: TM3 > TM6 > TM2 > TM7 > TM5 > TM1 > TM4.

Forrest and co-workers¹⁸ have suggested that plausible models of the TM regions of the membrane proteins can be obtained for the template: target sequence identities of $\geq 30\%$. Therefore, observed high-sequence identity between three subtypes of β -ARs further encouraged us to apply homology modeling techniques in the construction of the 3D model of human β_3 -AR. Recently, Mobarec et al.¹⁹ have suggested that the outer membrane TM segments of inactive GPCRs structures differ more than their corresponding inner membrane TM segments based on the comparison of the five available inactive 3D structures of GPCRs using global pairwise 3D structural alignments of the C_α atoms of their corresponding TM regions to calculate root-mean-square deviation (RMSD) values. Notably, in their analysis, the most similar GPCR structures resulted to be β_1 - and β_2 -ARs, which share a 68% sequence identity (Supporting Information) and a RMSD of 0.6 Å after superposition of 208 corresponding TM C_α atoms. Therefore, it may be concluded that preferential use of these two GPCRs namely β_1 - and β_2 -ARs over other GPCRs in the TM model building of β_3 -AR may be made. However, we preferred to use the human β_2 -AR structure bound to carazolol (PDB ID: 2rh1)¹² as template for the model development of human β_3 -AR structure due to the two facts viz.: (i) better atomic resolution (2.4 Å) of β_2 -AR, as compared to 2.7 Å of β_1 -AR (PDB ID: 2vt4) structures and (ii) the β_2 -AR structure bound to carazolol (PDB ID: 2rh1) is from human source, while the β_1 -AR (PDB-Id: 2vt4) is from turkey source.

Generation and Refinement of human β_3 -AR Model. A plausible homology model of the human β_3 -AR is generated using Modeller9v²⁰ considering a high-resolution crystal structure of human β_2 -AR (PDB ID: 2rh1)¹² determined at 2.4 Å resolution as template based on the ClustalW²¹ software-based sequence alignment (Figure 1). The global sequence identity and similarity between the human β_2 - and β_3 -ARs are 37.4 and 50.6%, respectively, which can be considered to be sufficient for generating reliable homology models.¹⁸ The sequence identity and

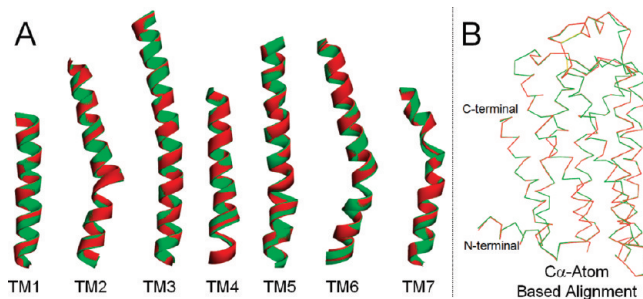


Figure 2. Backbone C_α helix atoms-based structural alignment of the human β₂- (PDB ID: 2rh1) and modeled β₃-AR: (A) alignment of seven TM helices; and (B) consensus C_α atom-based alignment of the two structures excluding ICL2. (β₂- and β₃-ARs are shown in red and green colors, respectively).

similarity between seven TMs of the two proteins (β₂- and β₃-ARs) increased to 59.9 and 75.8%, respectively. Also, the amino acids in the putative binding pocket, such as D^{3.32}, S^{5.42}, S^{5.43}, S^{5.46}, W^{6.48}, N^{7.39}, and Y^{7.43} are completely conserved, and hence their correct orientations are retrievable in the generated homology model of human β₃-AR. These facts further substantiate the suitability of human β₂-AR structure as a template for the generation of plausible homology model of human β₃-AR. Initially, manual and automated modeling procedures were considered for generating a number of human β₃-AR models with an ultimate aim to explore all possible topological arrangements for packing seven TMs into a compact bundle. Only those seven-helix bundle arrangements that corroborated with the experimentally determined putative binding site residues,^{14–17,22} such as D^{3.32}, S^{5.42}, S^{5.43}, S^{5.46}, W^{6.48}, N^{7.39}, and Y^{7.43}, in a localized region of the interior helices were selected for further refinement. This strategy afforded a small number of receptor models exhibiting energetically reasonable backbone conformations, stereochemistry, and side-chain packing interactions, while also forming plausible ligand-binding sites consistent with available experimental data.^{14–17,22} The resulting human β₃-AR models have further been subjected to multiple quality assessments (MQA) methods, namely Procheck,²³ ProQ,²⁴ and ProSA-web,²⁵ for final model selection and further refinements. Based on the data from various MQA methods (provided in Supporting Information), the best homology model, with no outlier in Procheck, LGscore (ProQ) of 4.13 (>4: extremely good model) and Z-score (ProsaWeb) of -5.03, is further refined with energy minimization and low-temperature (30 K) molecular dynamics with constrained backbone in order to relieve unfavorable steric clashes.

The resulting human β₃-AR model has highly symmetrical backbone conformations with that of the human β₂-AR and has acceptable stereochemical parameters and side-chain packing densities. The RMSD for backbone C_α helix atoms of human β₂- and β₃-ARs is 0.759 Å only (Figure 2). The RMSD for the backbone C_α helix atoms and main chain atoms of the seven TMs of the human β₂- (PDB ID: 2rh1) and modeled β₃-AR is summarized in Table 2. The RMSDs between each TM of the human β₂- and modeled β₃-ARs are very low, which further confirms the plausibility of the developed homology model.

Notable Model Characteristics. Highly conserved proline residues in GPCRs probably induce notable kinks in the TM helices and may serve important functional roles in signal transduction.²⁶ A set of five of total seven proline kinks in seven

Table 2. RMSD for Backbone C_α Helix Atoms and Main Chain Atoms of the Seven TM Helices of Human β₂- and Modeled β₃-AR^a

title	TM1	TM2	TM3	TM4	TM5	TM6	TM7
C _α atoms RMSD	0.086	0.062	0.073	0.094	0.092	0.083	0.082
main chain atoms RMSD	0.104	0.125	0.099	0.130	0.135	0.120	0.120

^a The RMSD is in Å and human β₂-AR PDB ID is 2rh1.

TMs are completely conserved between β₂- and β₃-ARs. The TM2, TM4, and TM6 of the β₂- and β₃-ARs comprised single proline kinks each, while TMs and TM7 comprised two proline kinks each. The proline kinks in TM2 (P92^{2.50}), TM4 (P172^{4.50}), TM5 (P216^{5.50}), TM6 (P307^{6.50}), and TM7 (P343^{7.50}) of the β₃-AR are completely conserved with the corresponding proline kinks in TM2 (P88^{2.50}), TM4 (P168^{4.50}), TM5 (P211^{5.50}), TM6 (P416^{6.50}), and TM7 (P451^{7.50}) of the β₂-AR.

Apart from the seven TM helices, β-ARs possess a short α-helical segment extending from the cytosolic end of TM7 that lies parallel to the lipid bilayer surface (Figure 3 and 5). Sequence alignment (Figure 1) suggests that these regions are also highly conserved between the three subtypes of β-ARs and hence are successfully generated in the β₃-AR model. Figure 4 shows the relative orientation of seven TM helices of the modeled β₃-AR on the extracellular and intracellular ends.

Intracellular, Extracellular Loop Regions and Ligand Binding Pocket: Comparative Analysis among Three Subtypes of β-ARs and Rhodopsin. Among the GPCRs, the most significant structural differences are in the extracellular loops and the ligand-binding regions. The β-adrenoceptors include three intracellular (ICL-1, ICL-2, and ICL-3) and three extracellular (ECL-1, ECL-2, and ECL-3) loops. The extracellular loops of β₂- and β₃-AR are very similar in terms of the helix arrangements and overall topology. The second extracellular loop (ECL-2) of β₁-, β₂- and β₃-ARs includes a set of four conserved cysteine residues. GPCRs are thought to exhibit a conserved disulfide link between the two extracellular cysteine residues in the top of TM3 and ECL2 (Figure 5). This is indeed found to be the case in the β-AR subtypes and in rhodopsin. The three cysteine residues in the ECL2 domain and one cysteine residue in the TM3 domain of β-ARs participate in the formation of two disulfide links, which are believed to be critical for stabilization of the ligand-binding pocket. In case of generated β₃-AR model, one disulfide bond was between TM3 and ECL2 (C110^{3.25} in TM3 and C196 in ECL2), while the second disulfide bond was intra-ECL2 domain (between C189 and C195) (Figure 5).

Figure 5 illustrates the comparison of the superimposed β₁-, β₂-, and β₃-AR structures, showing distinguishable features in the extra- and intracellular domains. The intracellular domains of β-ARs are similar in terms of helix arrangements and consensus topology except ICL2. The ICL2 domain of β₁-AR possesses a short α-helix, which is absent in β₂- and β₃-AR and also in the rhodopsin structure (Figure 5). The ICL2 domain of β₂- and β₃-AR is identical with respect to helix arrangements and local topology. The second extracellular loop (ECL2) of rhodopsin has a short β-sheet that caps covalently bound 11-cis-retinal, while the ECL2 domain of the three subtypes of β-ARs comprise a short α-helix being stabilized by intra- and interloop disulfide bonds. The highly conserved amino acids among most of the family A GPCRs exhibit an important common feature referred to as 'ionic lock'—a salt bridge between the charged residue R^{3.50}

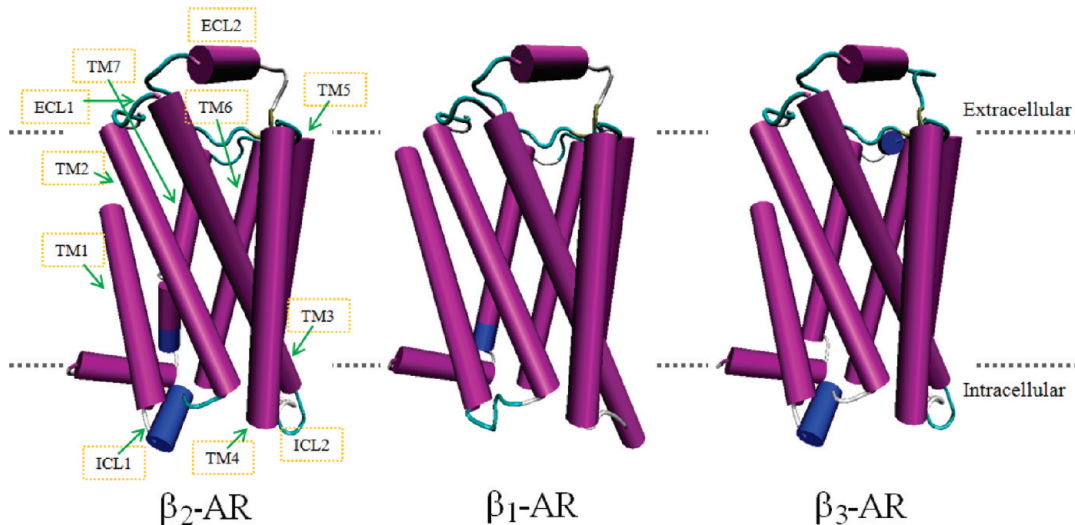


Figure 3. Annotation and comparative analyses of the three subtypes of β -adrenergic receptors in terms of the arrangements of seven TM helices, three intra- (ICL1–3) and three extra-cellular loops (ECL1–3).

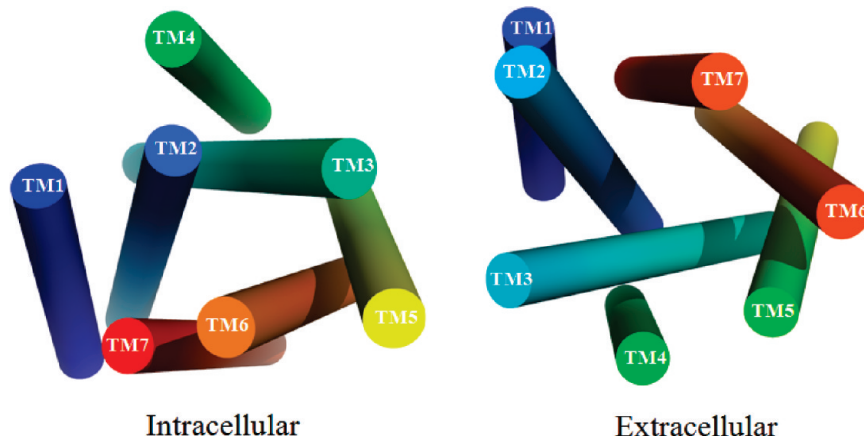


Figure 4. Top extracellular and intracellular stereoviews showing relative orientations of the seven TMs of the modeled $\beta_3\text{-AR}$. The three intra- (ICL1–3) and three extra-cellular loops (ECL1–3) along with an extra short helix next to the TM7 is not shown for better display.

in the conserved “[E]DRY” motif and the D/E^{6,30} at the cytoplasmic side of the two TM helices TM3 and TM6. This network of polar interactions was observed in all of the inactive rhodopsin crystal structures^{27,28} and has been well implicated through mutagenesis as a major factor in stabilizing the inactive state of GPCRs.^{29,30} Despite the presence of residues capable of forming this interaction, the ionic lock has not been established in any of the other GPCR crystal structures published to date.^{13,31–34} Since we have used the crystal structure of $\beta_2\text{-AR}$ (PDB ID: 2rh1) as a template, the broken ionic lock between 134^{3,49}–DRY–136^{3,51} and E286^{6,30} has also been observed in our modeled structure of $\beta_3\text{-AR}$ (Figure 5). Such a finding in all GPCRs crystal structures except rhodopsin is quite puzzling and has been thought to be partly attributable to the insertion of the T4L fusion protein within ICL3, which may induce a non-native helical conformation within this region.³⁵ Moreover, the absence of ionic lock in the recently discovered nanobody stabilized active-state crystal structure of $\beta_2\text{-AR}$ further forecasts the possibility of the broken ionic lock in the active state of GPCRs. The presence of broken ionic lock in our model (Figure 5)

substantiates its reliability for the study of structural basis for subtype selectivity among three β -adrenoceptors.

In the recent past, Daniel et al.³⁶ reported that cyanopindolol and carazolol bound to β_1 - and β_2 -receptors, respectively, are located slightly more extracellular than 11-cis-retinal bound to rhodopsin. Such positional disparities may be due to the differential interactions with the residues W286^{6,48} (in case of $\beta_2\text{-AR}$) and W303^{6,48} (in case of $\beta_1\text{-AR}$), which are proposed to undergo key rotamer conformational transitions in GPCR activation, referred as ‘rotamer toggle switch’. This conserved aromatic residue is W305^{6,48} in the modeled $\beta_3\text{-AR}$ and appears to undergo similar conformational transitions in the process of activation. Although, the partial agonism of β -ARs can be achieved by ligands without undergoing the toggle switch, but full agonism appears to involve this conformational change induced by the bound ligand. The ligand binding, both in the adrenergic receptors and rhodopsin, is mediated by polar and hydrophobic residues from TM domains TM3 and TM5–TM7. Previous investigations have demonstrated a critical role of a set of three residues, namely S203^{5,42}, S204^{5,43} and S207^{5,46} in the TM5 of the $\beta_2\text{-AR}$ for its

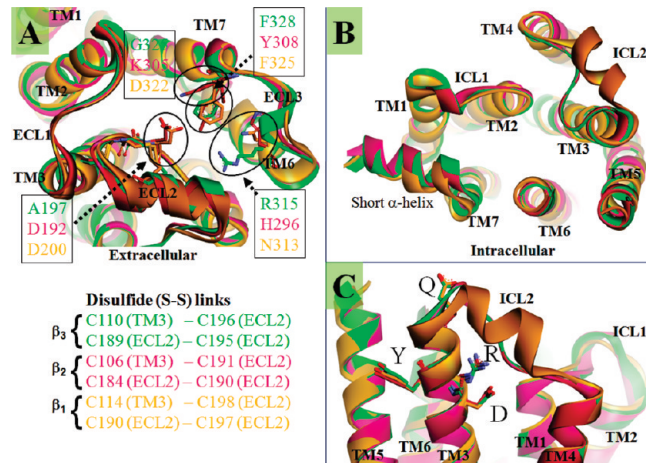


Figure 5. Comparison of superimposed β_1 -, β_2 -, and β_3 -AR structures shown as pink-, orange-, and green-colored ribbon, respectively. These two structures were aligned using the maestro align function. (A) the extracellular top-view showing distinguished features in the extracellular ligand binding domains of the three β -adrenoceptors; (B) the intracellular stereoview showing the presence of a short helix in ICL2 of β_1 - shown in orange; and (C) side intracellular view of TM domains showing the ionic lock interaction between Asp and Arg of the DRY motif in TM3 is broken.

partial agonism.³⁷ Sequence alignment of three subtypes of β -ARs indicates that these three residues in the TMs are completely conserved in the three subtypes of β -receptor and represent β -receptor microdomain that is involved in the hydrogen bonding (H-bonding) with the catechol hydroxyl groups of catecholamines (epinephrine and norepinephrine; their chemical structures are given as Supporting Information). While two serines S203^{5,42} and S204^{5,43} exhibit a bifurcated hydrogen bond (H-bond) with the meta-OH, the third serine S207^{5,46} interacts with para-OH of catecholamines.³³ Thus, it may be stated that these residues are fundamental for β_3 -AR agonism by the catechol class of small molecules. As described above, the sequence identity and similarity between seven TMs of β_1 - and β_3 -ARs are 61.2 and 75.3%, respectively, whereas between β_2 - and β_3 -ARs were 59.9 and 75.8%, respectively. The high-sequence similarity for these three receptor subtypes suggests that they must possess quite similar 3D topological as well as helix arrangements. Also, the binding site residues in each receptor subtype must also have extremely similar structures and hydration characteristics, since the residues lining the binding site region of the three receptors are nearly identical with sequence identity of 75–85%. Despite the extremely high-sequence similarity for all three receptor subtypes, there is growing evidence that the β_3 -AR may bind ligands to some extent differently than β_1 - and β_2 -receptors. Based on the analysis of binding site residues in the three β -adrenoceptors (β_1 , β_2 , and β_3), we found that these TM6 residues are N313^{6,58} in β_1 , H296^{6,58} in β_2 , and R315^{6,58} in β_3 -AR, which differ significantly in terms of their overall size, charge density, and overall capability to form H-bonds with the neighboring residues or ligands. Previously, based on ligand-binding measurements for a number of β -receptor chimeras and site-directed mutants, Kikkawa et al.³⁸ suggested that a single aromatic residue Y308^{7,35} in the extracellular end of TM7 in the β_2 -AR is responsible for β -receptor subtype selectivity. This residue is F325^{7,35} in β_1 and F328^{7,35} in β_3 -AR. In the ECL2 domain adjacent to the conserved disulfide bond to TM3 of our

β_3 -AR model, few more notable differences are: (i) the presence of hydrophobic residue A197 in place of D192 in β_2 and D200 in β_1 -ARs, (ii) the presence of H93^{2,55} in the TM2 of β_2 in place of L101^{2,55} in β_1 and L97^{2,55} in β_3 -ARs, and (iii) the presence of G325 in ECL3 domain of β_3 in place of D322 in β_1 and K305 in β_2 -AR.

Binding Modes of Selective β_3 -AR Agonists and Antagonists: Rationale for Subtype-Selectivity. Development of a number of impressive β_3 -AR selective ligands forecasts the existence of exploitable differences in the three subtypes of β -receptor. It is also interesting to note that most of β_3 -AR selective ligands did not share the catechol core of epinephrine; rather they comprised either a pyrimidine or *m*-chlorobenzyl ring and hence additionally suggested that these ligands may have unique binding modes within the binding pocket of the β_3 -AR that furnishes the selectivity over other two subtypes (β_1 - and β_2 -).

In order to investigate the binding modes of different β -receptor ligands and their molecular recognitions in different local and/or distal microdomains leading to the particular subtype-selectivity, a diverse class of reported potent and selective β_3 -AR agonists, covering most of the reported chemotypes^{39–50} (Figure 6), and the only one selective antagonist⁵¹ were chosen for systematic docking studies into the binding site of homology modeled β_3 -AR using Glide⁵² module implemented in Schrödinger⁵³ package. In addition, these ligands were also docked and scored into the binding site of high-resolution crystal structures of β_1 - and β_2 -AR and then compared with the poses of these ligands into the binding site of β_3 -AR. In general, the binding sites for the β -receptor ligands (both agonists and antagonists) are contained in a deeply buried binding pocket formed by the TM helices as evidenced by X-ray crystallographic of the inverse agonist carazolol bound to the β_2 -AR,¹² full agonist bound to the β_2 -AR,¹³ and antagonist bound to the β_1 -AR.³⁴ The amino acid residues that are directly involved in the binding with the agonists and THE antagonists are localized in the TM helices (TM3 and TMS-TM7) and the ECL2 loop domain. The microscopic binding of each agonist within the active site of the β_1 -, β_2 -, and β_3 -ARs was examined and ranked based on the glidescore, a scoring function implemented in Schrödinger package, as well as based on the different experimentally derived information. The binding poses of these ligands into the active site of β_1 - and β_2 -ARs are provided as Supporting Information.

Selective β_3 -AR Agonists:^{39–50} The complexes of representative β_3 -AR selective agonists are depicted in Figures 7–9. The overall binding modes of the selective agonists were comparable in terms of their relative disposition in the deeply buried binding pocket and interactions with the surrounding residues of the localized TM helices. The visual inspection of the complexes revealed that all the microscopic binding structures exhibit some H-bonds and/or hydrophobic (π – π and/or cation– π) interactions. The details of the bindings of the selective β_3 -agonists into the binding pocket of β_3 -AR are summarized in Table 3. The energetically favored and nearly common interactions among all agonists and the classical small molecule transmitter (epinephrine) are: (i) salt bridge between the protonated amine, the carboxylated side chain of D117^{3,32}, and the carbonyl oxygen of the N332^{7,39} and (ii) a salt bridge between the β -hydroxyl and the amine terminal of N332^{7,39}. These two residues D117^{3,32} and N332^{7,39} are completely conserved among the biogenic amine receptors, and also the central β -hydroxylethylamine is also present in all the reported full/partial agonists, inverse agonists, and antagonists as well as the classical small molecule transmitters

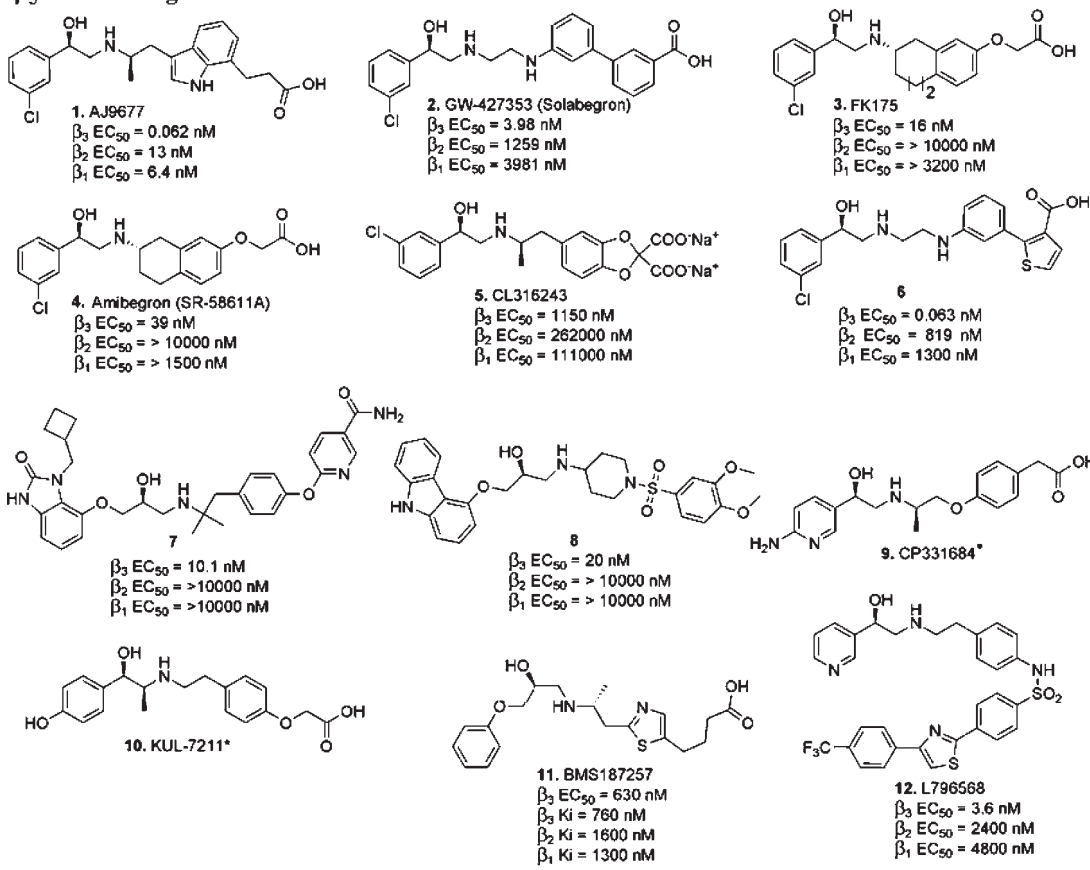
β_3 -Selective Agonists

Figure 6. Highly selective β_3 -AR agonists (1–12) and antagonist (13) covering wide structural diversity collected from the literature.^{39–50} *Agonistic/antagonistic activities not found in the literature.

(epinephrine). The only difference was the tightness of binding (geometric distances) of ligand with these residues, D117^{3,32} and N332^{7,39} in the deep binding pocket.

Our observations well corroborate with the previous experimental results, such as the point mutation of the hamster β_2 -AR revealing the vitality of a key amino acid residue D113^{3,32} for high-affinity binding of both agonists and antagonists⁵⁴ and the critical role of N312^{7,39} of the β_2 -AR in TM7 in the stereoselective interaction with the β -hydroxyl group of β -AR ligands.⁵⁵ One additional three point H-bond interaction has been observed between Y336^{7,43} in the TM7, the protonated amine, and β -hydroxyl group in most of the referred selective agonists, which has not been observed with small molecule signaling transmitters, epinephrine, and norepinephrine (Figures 7–9). This critical observation is substantiated by the very recent publication on the nanobody stabilized active-state structure of β_2 -AR bound to the full agonist, where the involvement of Y316^{7,43} in interaction with protonated amine of the full agonist is reported.¹³ Since most of the selective β_3 -AR agonist (Figure 6) do not share the catechol core of epinephrine, the strong H-bonding with the surrounding polar residues (serines)

in the deeply buried binding pocket were partly absent in most of the selective β_3 -AR agonists, although it was previously demonstrated to be critical for the partial agonism of β_2 -AR. Thus, it may be stated that the polar interactions with these residues are not critical for the selective activation of the β_3 -receptor. The aromatic ring attached to the β -hydroxyl chiral carbon was stabilized in the deep binding pocket of the receptor by the strong array of hydrophobic contacts with the residues, namely W305^{6,48}, F308^{6,51}, and F309^{6,52} from the aromatic wall region of TM6 and with residues V118^{3,33} and V121^{3,36} located in TM3 domains (Figure 7–9). The arylpropanolamine class of selective agonists, such as compound 7 (β_3 -AR EC₅₀ = 10.1 nM), 8 (β_3 -AR EC₅₀ = 20 nM), and BMS187257 (β_3 -AR EC₅₀ = 630 nM), penetrated relatively better in this region, and the in-between hydrophobic contacts were strengthened proportionately with the increase in the bulkiness of the aryl group of the agonist. For example, the cyclobutylmethyl group attached to N1-position of 1H-benzo[d]imidazol-2(3H)-one ring system in the compound 7 was engaged in strong hydrophobic interactions with the surrounding hydrophobic microdomain of TM3 and TM6, which led this compound with considerably better affinity

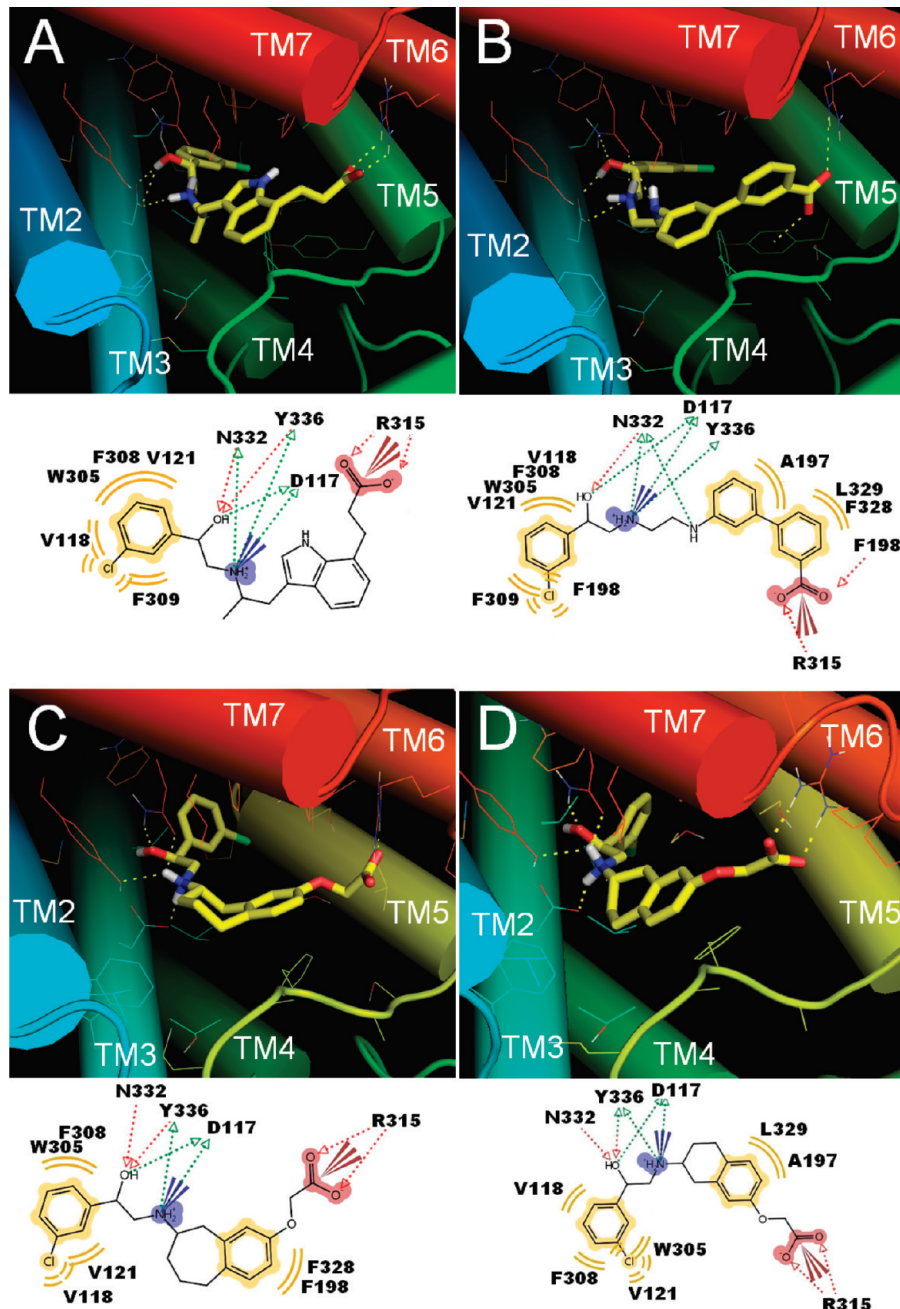


Figure 7. Close-up extracellular stereoviews of the β_3 -agonists: (A) AJ9677, (B) solabegron, (C) FK175, and (D) amibegron complexed with the homology modeled β_3 -AR, displayed in schematic cartoon form. The ligand is displayed in yellow stick form, and key binding site residues are shown in line form. H-bonds are represented with dashed yellow lines. Schematic 2D plots of intermolecular interactions observed for complexes are shown on the bottom.

than the other two agonists, namely compound 8 and BMS-187257, possessing 9H-carbazol and phenoxy groups, respectively, at the corresponding position next to β -hydroxyl group. The relatively poor affinity of the BMS187257 compared to the compound 8 was due to the lack of any small hydrophobic group substituted to the phenyl ring. Such a hydrophobic group of relatively small bulk was found to be essential for tightly binding and stabilization into the deep binding pocket of β_3 -receptor and thus for obtaining high-affinity β_3 -receptor agonists. In case of arylethanolamine class of selective agonists, such as AJ9677 (β_3 -AR EC₅₀ = 0.062 nM), solabegron (β_3 -AR EC₅₀ = 3.98

nM), amibegron (β_3 -AR EC₅₀ = 39 nM), etc., the m-chlorophenyl groups being directly attached to the β -hydroxyl carbon exhibited strong hydrophobic contacts with the surrounding aromatic and nonaromatic residues, namely W305^{6,48}, F308^{6,51}, F309^{6,52}, V118^{3,33}, and V121^{3,36} (Figures 7–9). In these agonists, the presence of a small hydrophobic chloro group successfully fulfilled the necessity mentioned above and thus resulted in high-affinity β -receptor agonists. Some selective agonists, such as compound 8, CP331684, and KUL7211, exhibited direct H-bonding interaction with one polar residue S211^{5,46}, which is conserved among three subtypes of β -adrenergic receptors. The coverage of hydrophobic

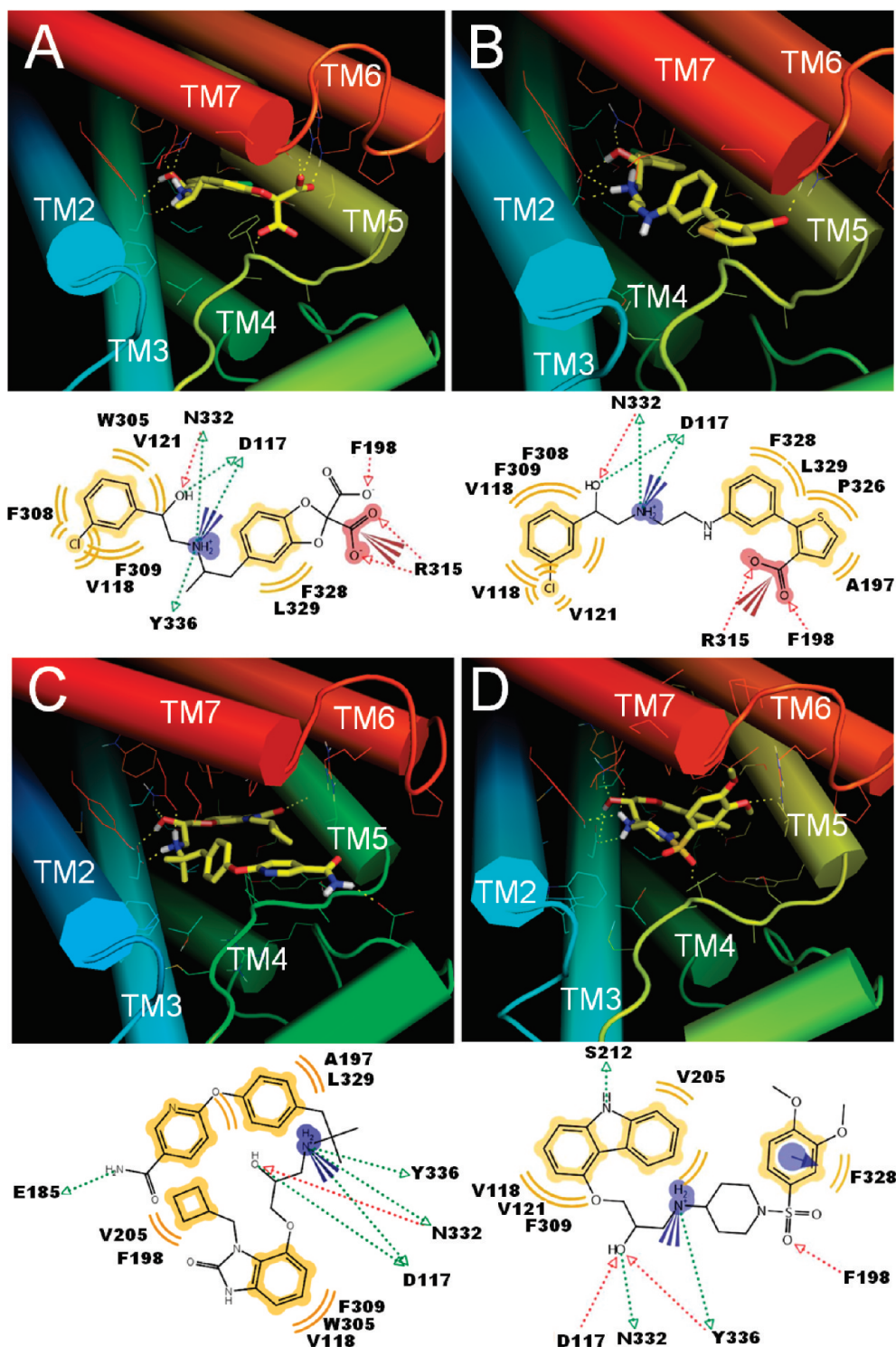


Figure 8. Close-up extracellular stereoviews of the β_3 -agonists: (A) CL316243, (B) compound 6, (C) compound 7, and (D) compound 8 complexed with the homology modeled β_3 -AR, displayed in schematic cartoon form. The ligand is displayed in yellow stick form, and key binding site residues are shown in line form. H-bonds are represented with dashed yellow lines. Schematic 2D plots of intermolecular interactions observed for complexes are shown on the bottom.

residues (F308^{6,51}, V118^{3,33}, and V121^{3,36}) around m-chloro of selective agonists, such as AJ9677, solabegron, amibegron, etc., suggests that bulkier groups at this position are favorable for better binding in this region, which may in turn facilitate the direct salt-bridge formation of the protonated amine and β -hydroxyl groups

with the completely conserved residues, namely D117^{3,32} and N332^{7,39}. Broadly, it may be stated that the hydrophobic residues (W305^{6,48}, F308^{6,51}, F309^{6,52}, V118^{3,33}, and V121^{3,36}) and ionizable residues (D117^{3,32} and N332^{7,39}) provide a three point positional constraint, which dramatically limits the degree of

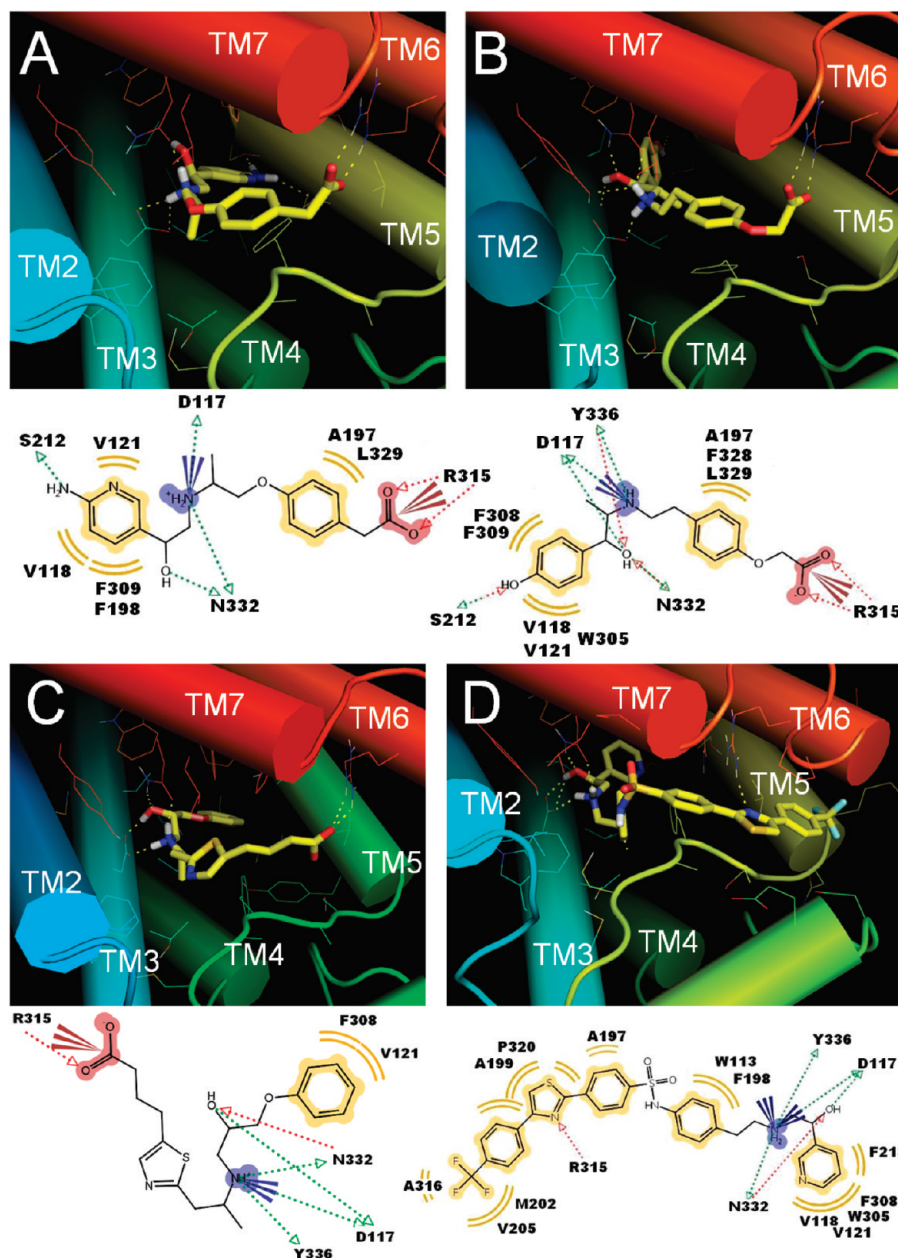


Figure 9. Close-up extracellular stereoviews of the β_3 -agonists: (A) CP331684, (B) KUL7211, (C) BMS187257, and (D) L796568 complexed with the homology modeled β_3 -AR displayed in schematic cartoon form. The ligand is displayed in yellow stick form, and key binding site residues are shown in line form. H-bonds are represented with dashed yellow lines. Schematic 2D plots of intermolecular interactions observed for complexes are shown on the bottom.

conformational and rotational freedom of the ligand in the binding pocket of β -ARs. In addition, Y336^{7,43} serves as hook for better fitting in the deep binding pocket formed by TM3 and TM5–TM7 of the receptor.

Among the reported selective agonists, unusual structural variations are observed in the groups attached to the protonated amine, and the same is observed in their orientations in the extracellular part of the binding pocket of β -ARs. One of the most potent and selective β_3 -AR agonists, e.g., AJ9677, comprises an unusual indol-7-yloxy acetic acid functionality attached to the protonated amine center, while another selective potent β_3 -AR agonist 6 possesses 2-phenyl-thiophene-3-carboxylate groups. Here, it may be stated that there are some specific molecular

recognition exist in the extracellular end of the TM helices, which induce the process of GPCR activation and signaling. The docking and scoring of minimized conformations of these selective β_3 -AR agonists suggest that while the centric β -hydroxylethylamine core remains interacting with the above stated conserved residues, namely D117^{3,32} and N332^{7,39} and that the aryl or aryloxy groups next to β -hydroxyl group remain embedded in the deep binding pocket formed by the aromatic and aliphatic residues (W305^{6,48}, F308^{6,51}, F309^{6,52}, V118^{3,33}, and V121^{3,36}), the unusual indol-7-yloxy acetic acid functionality of AJ9677, attached to the protonated amine center, occupies the extracellular region of TM3, TM6, and TM7 favorably, where the ligand carboxylate group forms a strong bifurcated H-bonding

Table 3. Summary of the Microscopic Binding of the Selective β_3 -Agonists into the Binding Site of β_3 -AR

title	β_3 -AR EC ₅₀ (nM)	β_3 -AR pEC ₅₀ (M)	glidescore			interacting residues ^d		
			SP ^b	XP ^c	TM3	TM5	TM6	TM7
Aj9677	0.062	10.208	-9.132	-11.071	V118 ^{3,33} , D117 ^{3,32}	—	W305 ^{6,48} , F308 ^{6,51} , F309 ^{6,52} , R315 ^{6,58}	N332 ^{7,39} , Y336 ^{7,43}
solabegron	3.98	8.400	-8.945	-10.971	V118 ^{3,33} , V121 ^{3,36} , D117 ^{3,32}	—	W305 ^{6,48} , F308 ^{6,51} , R315 ^{6,58}	L329 ^{7,36} , N332 ^{7,39} , Y336 ^{7,43} , A197, F198
FK175	16	7.796	-8.854	-10.577	V118 ^{3,33} , V121 ^{3,36} , D117 ^{3,32}	—	W305 ^{6,48} , F308 ^{6,51} , R315 ^{6,58}	F328 ^{7,35} , L329 ^{7,36} , N332 ^{7,39} , Y336 ^{7,43} , F198
amibegron	39	7.409	-8.890	-10.457	V118 ^{3,33} , V121 ^{3,36} , D117 ^{3,32}	—	W305 ^{6,48} , F308 ^{6,51} , R315 ^{6,58}	L329 ^{7,36} , N332 ^{7,39} , A197
CL316243	1150	5.939	-8.516	-9.473	V118 ^{3,33} , V121 ^{3,36} , D117 ^{3,32}	—	W305 ^{6,48} , F308 ^{6,51} , F309 ^{6,52} , R315 ^{6,58}	F328 ^{7,35} , L329 ^{7,36} , N332 ^{7,39} , Y336 ^{7,43} , F198
6	0.063	10.201	-8.135	-10.645	V118 ^{3,33} , V121 ^{3,36} , T122 ^{3,37} , D117 ^{3,32}	—	W305 ^{6,48} , F308 ^{6,51} , R315 ^{6,58}	F328 ^{7,35} , L329 ^{7,36} , N332 ^{7,39} , A197, F198, E185
7	10.1	7.996	-11.227	-12.320	V118 ^{3,33} , D117 ^{3,32}	V205 ^{5,39}	W305 ^{6,48} , F308 ^{6,51}	L329 ^{7,36} , N332 ^{7,39} , A197, F198, E185
8	20	7.699	-11.148	-12.859	V118 ^{3,33} , V121 ^{3,36} , D117 ^{3,32}	V205 ^{5,39} , S211 ^{5,46}	F309 ^{6,52}	P326 ^{7,33} , F328 ^{7,35} , N332 ^{7,39} , Y336 ^{7,43} , A197, F198
CP331684 ^a	—	—	-7.338	-9.000	V118 ^{3,33} , V121 ^{3,36} , D117 ^{3,32}	S211 ^{5,46}	F309 ^{6,52} , R315 ^{6,58}	F328 ^{7,35} , L329 ^{7,36} , A197, F198
KUL7211 ^a	—	—	-8.554	-9.689	V118 ^{3,33} , V121 ^{3,36} , D117 ^{3,32}	S211 ^{5,46}	W305 ^{6,48} , F308 ^{6,51} , F309 ^{6,52} , R315 ^{6,58}	F328 ^{7,35} , L329 ^{7,36} , N332 ^{7,39} , Y336 ^{7,43} , A197, F198
BMS187257	630	6.201	-8.069	-11.806	V118 ^{3,33} , D117 ^{3,32}	—	F309 ^{6,52} , R315 ^{6,58}	N332 ^{7,39} , Y336 ^{7,43}
L796568	3.6	8.444	-9.991	-10.789	W113 ^{3,27} , V118 ^{3,33} , V121 ^{3,36} , D117 ^{3,32}	V205 ^{5,39} , M202 ^{5,36} , F213 ^{5,47}	W305 ^{6,48} , F308 ^{6,51} , R315 ^{6,58}	N332 ^{7,39} , Y336 ^{7,43} , A197, F198, A199, P320

^a β_3 -AR EC₅₀ not found. ^b Standard precision. ^c Extra precision. ^d Important amino acids of the binding pocket found interacting in terms of direct H-bond or electrostatic or hydrophobic.

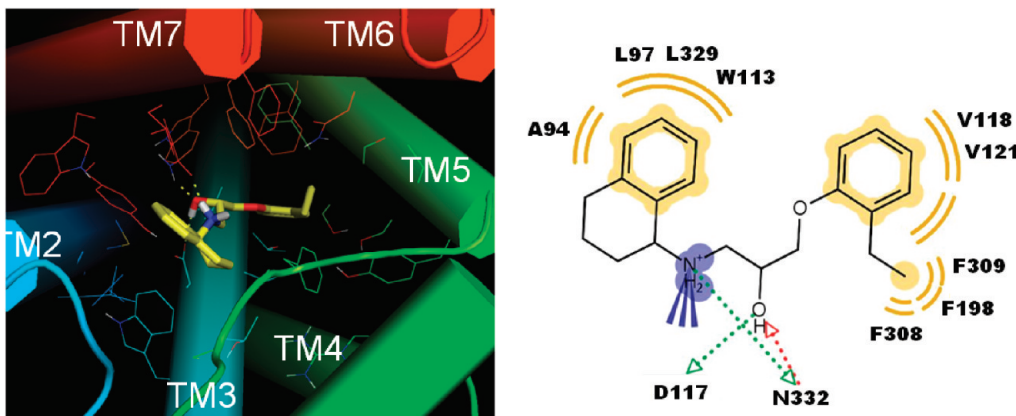


Figure 10. Close-up extracellular stereoview of the β_3 -antagonist SR-59230A complexed with the homology modeled β_3 -AR, displayed in schematic cartoon form. The ligand is displayed in yellow stick form, and key binding site residues are shown in line form. H-bonds are represented with dashed yellow lines. Schematic 2D plots of intermolecular interactions observed for complexes are shown on the bottom.

with R315^{6,58}, and the indole ring exhibits an edge-to-face contact with the F198 of extracellular ECL2 loop. This loop ECL2 delineates the entrance of the ligand-binding pocket and is stabilized by two disulfide bonds being conserved in the three β -adrenoceptors. Similar interactions are observed with other potent β_3 -AR ligands having negatively ionizable centers, such as solabegron, amibegron, FK175, compound 8, CP331684, BMS187257, and KUL7211, etc. (Figures 7–9). Most of these selective agonists possess a terminal carboxylate group that is involved in the charge-reinforced, bifurcated H-bonding with the positive ionizable residue R6.30 located in TM6 of β_3 -AR. Moreover, one noncarboxylate selective agonist L796568, possessing thiazole functionality, also was found to exhibit direct monodentate H-bonding interaction with R315^{6,58} of the β_3 -AR (Figure 9D). This positively ionizable residue R315^{6,58} is not conserved among the three subtypes of β -receptors and thus represents one of the selectivity governing residues for the reported β_3 -selective agonists. These nonconserved residues are H296^{6,58} in β_2 - and N313^{6,58} in β_1 -ARs (Figure 1), which differ significantly from β_3 -specific R315^{6,58} residue in terms of their overall size, charge density, protonation potential, and overall capability to form H-bond with the neighboring residues or ligands. Moreover, the residue R315^{6,58} can form much stronger local (direct) and long-range electrostatic interactions with the localized residues or the acidic groups of the bound ligands compared to the N313^{6,58} and H296^{6,58} present in β_1 - and β_2 -ARs, respectively. Moreover, as previously stated by Kikkawa et al, the presence of Y308^{7,35} in β_2 , in place of F325^{7,35} and F328^{7,35} in β_1 - and β_3 -ARs, respectively, is also one of the critical factors which limit the exposure of the negatively ionizable carboxylate center to interact with the H296^{6,58} of the β_2 -AR due to relatively greater steric hindrance with the hydroxyl group of Y308^{7,35} and thus explaining the better agonistic activity of these selective agonists toward β_1 - and β_3 - over β_2 -ARs.

Although most of these selective agonists (Figure 6) have at least one negatively ionizable center, noticeable differences do exist in the linkers connecting the protonated secondary amine and the negatively ionizable carboxylate functionalities. Most of these agonists possess a ring aromatic center as a part of linker present at almost comparable distance (2–3 carbon distances) from the protonated amine center. Although, the overall location of this aromatic ring is comparable in the extracellular end of the binding pocket near ECL2 domain of both β_1 - and β_3 -ARs, but

there is some steric perturbation in the binding site of β_2 -AR due to the presence of relatively bulkier residue Y308^{7,35} in TM7, suggesting it to be one of the limiting factor for the exposure of the negatively ionizable carboxylate center to interact with the H296^{6,58} present in the β_2 -AR. The conserved residue F198 in the ECL2 domain of β -receptor subtypes serves as the bottom support to the linker aromatic ring for the favorable charge reinforced H-bonding with the positively ionized residue R315^{6,58} in TM6 of the β_3 -AR. The linkers of the β_3 -selective agonists also experience strong hydrophobic contacts with the F328^{7,35} and L329^{7,36} residues in the β_3 -receptor. These residues are not conserved in all β -receptors and correspond to F325^{7,35} and V326^{7,36} in β_1 - and Y308^{7,35} and I309^{7,36} in β_2 -receptors. Additionally, β_3 -specific residue A197 in the ECL2 domain of the β_3 -receptor corresponds to the aspartic acid residue in both β_1 - (D200) and β_2 - (D192) receptors (Figure 1). The presence of these acidic residue D200 and D192 in β_1 - and β_2 , combined with the lack of a compelling protonated basic partner N313^{6,58} and H296^{6,58} in β_1 - and β_2 -AR, respectively, for the interaction with the carboxylate group present in most of the β_3 -selective ligands and the obstruction by the nonconserved residues Y308^{7,35} in β_2 - in TM7 domain, suggests a possible basis for the higher affinity of these selective ligands for β_3 - over β_1 - and β_2 -ARs.

β_3 -AR Antagonist. The docked pose of β_3 -AR selective antagonist (SR-59230A, Figure 6)⁵¹ in the modeled β_3 -AR structure is shown in Figure 10. The β_3 -AR model is observed to comfortably accommodate the selective antagonist in the deep binding site, where the residue N332^{7,39} exhibits stereoselective H-bonding with both the β -hydroxyl and protonated amino groups and the residue D117^{3,32} H-bonded to the β -hydroxyl group of the SR-59230A. It has been documented earlier that the stereoselective binding of aryloxypropanolamine antagonists may be determined by N332^{7,39} residue being conserved in the three β -receptor subtypes. Mutation of N312^{7,39} in the β_2 -AR reduces the binding of both agonists as well as antagonists considerably,⁵⁶ and the mutation of the equivalent residue N385^{7,39} in the human serotonin 5-HT_{1A} receptor abolishes the stereoselective binding of β_2 -antagonists.⁵⁷ In addition, Frielle et al.⁵⁸ reported that TM6 and TM7 of β -ARs play a significant role in determining the binding of the β_1 - and β_2 -selective antagonists, such as betaxolol and ICI-118551. These mutational data suggest that the deleterious agonist and

antagonist binding, affected by the N312^{7,39} mutation in β_2 -AR, may be due to the structural perturbations created in the binding site.

The aryloxy groups attached to the β -hydroxyl carbon are more extended and bulkier in most of the β -blockers. This part of antagonist penetrates into the deep binding pocket comparatively to greater extent ($\sim 2 \text{ \AA}$) than the agonists and is involved in the strong hydrophobic interactions with the surrounding residues (Figure 10). The phenyl ring of β_3 -AR selective antagonist SR-59230A exhibits hydrophobic contacts with a set of three residues, namely V118^{3,33}, V121^{3,36}, and F308^{6,51}, while *o*-ethyl group attached to the phenyl ring is being extended in the deep pocket toward the extracellular region experiencing strong hydrophobic contacts with F309^{6,52} and F198 (ECL2) residues of the β_3 -AR. The unique and bulkier 1,2,3,4-tetrahydronaphthalene group attached to the protonated amine fits well in the extracellular portions of the binding site and is surrounded by the hydrophobic residues of TM2, TM3, and TM7. The aromatic ring of this unique group exhibits strong hydrophobic contacts with the A94^{2,52}, L97^{2,54}, W113^{3,28}, and L329^{7,36} residues of the β_3 -AR. Unlike the agonist binding (discussed above), the selective antagonist orients itself more closely to the TM2 and TM3 and is measurably far away from the TM6 residue R315^{6,38} due to the lack of any negatively charged center or heteroatom in the substituent attached to the protonated amine of the antagonist. Our modeling results do indicate that the antagonist binding with the β -ARs is fairly different from that of agonist binding and makes unique hydrophobic contacts with TM2 residues. However, more experimental studies are needed for the understanding of the antagonist–receptor binding in greater details.

Our homology model has comfortably accommodated a wide variety of ligands (agonists and antagonists) and has well explained the activity variation among the reported wide class of selective agonists in terms of their specific interactions with the binding site residues and their relative disposition in the deeply buried binding site surrounded by the seven TMs. Broadly, it was found that residues of TM3, TM6, TM7, and ECL2 domains play vital role in governing high-affinity and subtype selectivity among the reported β -receptor agonists. The subtype-specific binding affinity of subtype-specific ligands seems to be due to influences on the spatial arrangements of these binding site residues as a result of conformational preferences in more distant residues in the outer TM helices as well as extracellular surfaces. The β_3 -receptor selective agonist must extend toward the extracellular opening of the binding pocket near the ECL2 domain and must form mono/bidentate H-bonds with the one of the most important and distinct protonated residue R315^{6,38} present in the TM6 of β_3 -AR.

Agonist–Receptor Binding Free Energy Calculations. To understand molecular recognition of protein surfaces, it is important to obtain the quantitative contributions of the individual forces governing binding affinity and specificity. The binding free energies (ΔG_{bind}) are calculated using Prime MM-GBSA module implemented in Schrödinger⁵³ package considering the complexes of agonists with modeled β_3 -AR and with high-resolution structures of β_1 and β_2 -ARs. Liaison⁶⁰ is also used to calculate structure-based descriptors by running MM simulations of the agonist–receptor complex and of the free ligand and free receptor, with the surface generalized Born (SGB) continuum solvation model. In the Prime MM-GBSA, MM-GBSA is an acronym for a method that combines optimized potentials for liquid simulations (OPLS) molecular mechanics energies (E_{MM}),

an SGB solvation model for polar solvation (G_{SGB}), and a nonpolar solvation term (G_{NP}). The G_{NP} term comprises the nonpolar solvent accessible surface area and van der Waals interactions. The total free energy of agonist binding (ΔG_{bind}) is then expressed as

$$\Delta G_{\text{bind}} = G_{\text{complex}} - (G_{\text{protein}} + G_{\text{ligand}}) \quad (\text{Eqn-1})$$

$$G = E_{\text{MM}} + G_{\text{SGB}} + G_{\text{N}} \quad (\text{Eqn-2})$$

where G is the summation of OPLS molecular mechanics energies (E_{MM}), the SGB solvation model for polar solvation (G_{SGB}), and a nonpolar solvation term (G_{NP}) comprising the nonpolar solvent accessible surface area and van der Waals interactions, G_{complex} is the total energy of the complex, G_{protein} is the energy of the receptor without the ligand, and G_{ligand} is the energy of the unbound ligand. The ligand in the unbound state is minimized in SGB solvent but is not otherwise sampled. In the calculation of the complex, the ligand is minimized in the context of the receptor.

Principally, the ligand–receptor binding is encouraged by the interaction between the charged centers of the ligand and the oppositely charged residues of the receptor, along with the localized and distant hydrophobic π – π and cation– π interactions. Hence, the binding free energy for an agonist structure binding with the receptor is the sum of contributions from both the local receptor–ligand binding within the binding pocket and the long-range electrostatic interactions between the charged agonist and the oppositely charged protein environment within/outside the binding pocket. When the energetic contributions from the local binding are close, the contributions from the long-range electrostatic interactions may have greater impact on the different binding of the charged ligands to the receptor. Specifically, for all of the agonists considered in this study, the binding free energies are calculated for the charged structures being docked into the binding pocket of the modeled β_3 -AR receptor using the Glide module.

The complex, ligand, and binding free energies along with the Liaison descriptors of the different agonist– β_3 -AR complexes based on Prime MM-GBSA calculations are summarized in Table 4. Furthermore, the above parameters were also computed for the considered agonists bound to the β_1 and β_2 -ARs. Figure 11 illustrates a graphical plot of the binding free energies of the considered agonists into the binding sites of β_1 -, β_2 -, and β_3 -ARs. As evident from the Figure 11, the estimated binding affinities of these ligands into the binding site of β_1 - and β_2 -ARs are considerably lower than those for β_3 -AR. This further suggests that the binding affinities of these ligands are considerably higher for β_3 - compared to β_1 - and β_2 -ARs.

In fact, the availability of the experimental binding free energies of these representative β -agonists upon binding with β -receptor may aid in studying the overall agreement with the calculated binding free energies (Table 4). However, the previous reports⁶¹ by different research groups suggest good agreement between the experimentally determined and the calculated binding free energies. In order to understand the quantitative contributions of the individual forces governing binding affinity and specificity of the β -receptor ligands considered in the present study, the interparameter correlations study has been carried out between the observed pEC_{50} (dependent variable) and the various individual forces generated using Liaison and Prime MM-GBSA modules based on the different agonist–receptor

Table 4. Liaison Descriptors, Free Energy, and Its Components for the Binding of the β -Agonists to the Modeled β_3 -AR

title	liaison descriptors					prime MM-GBSA end-point free energies ^a							
	U_{vdW}	U_{Coul}	U_{rxnf}	U_{cav}	U_{ele}	G_{complex}	G_{ligand}	ΔG_{bind}	ΔG_{Coul}	ΔG_{Cov}	ΔG_{vdW}	$\Delta G_{\text{Solv SA}}$	$\Delta G_{\text{Solv GB}}$
AJ9677	-47.19	-254.19	88.60	1.19	-76.99	20190.28	-113.91	-52.80	-95.59	3.64	-46.36	-1.19	86.70
solabegron	-48.72	-231.44	48.18	2.93	-135.08	20200.82	-111.44	-44.73	-46.40	0.96	-45.47	1.12	45.06
FK175	-39.98	-262.23	103.61	1.38	-55.02	20237.91	-86.87	-32.21	-110.24	10.19	-34.33	-1.47	103.64
amibegron	-37.71	-262.36	105.81	1.15	-50.75	20216.02	-95.47	-45.50	-112.14	8.45	-35.89	-0.14	94.22
CL316243	-43.23	-297.05	147.35	1.66	-2.35	20283.52	-44.14	-29.34	-140.15	2.39	-47.12	-1.43	156.97
6	-47.84	-215.93	33.81	3.28	-148.32	20221.45	-109.79	-25.75	-14.49	-4.71	-46.43	-0.35	40.23
7	-63.84	-222.72	76.70	5.02	-69.32	20250.18	-48.07	-58.75	-94.82	12.45	-41.30	3.11	61.82
8	-60.78	-184.70	65.92	3.06	-52.85	20277.50	-31.69	-47.80	-73.86	16.39	-47.87	2.77	54.77
CP331684	-33.94	-256.91	104.62	2.89	-47.66	20164.91	-142.00	-50.08	-113.70	4.00	-42.70	0.03	102.29
KUL7211	-77.02	-207.41	75.37	2.24	-56.66	20211.51	-80.29	-65.20	-76.12	2.14	-54.03	2.28	60.54
BMS187257	-39.66	-239.02	87.27	0.62	-64.49	20175.91	-124.32	-56.77	-98.05	3.47	-47.75	-0.53	86.11
L796568	-72.16	-184.53	70.99	2.24	-42.56	20244.06	-78.57	-34.36	-50.59	16.40	-60.95	3.81	56.97
correlation (R) ^b	0.249	0.365	0.656	0.290	0.676	0.292	0.474	0.721 ^c	0.663	0.224	0.114	0.077	0.608
R^2	0.062	0.133	0.430	0.084	0.457	0.085	0.225	0.520	0.440	0.050	0.013	0.006	0.370

^a All reported energies are in kcal/mol. Total energy of the β_3 -receptor (G_{Receptor}) was 20356.99 kcal/mol. ^b Correlation between individual forces and the observed agonistic pEC_{50} for 10 compounds. Please note that the two compounds CP331684 and KUL7211 were excluded from the correlation study due to the unavailability of their agonistic activities; U_{vdW} : the van der Waals energy; U_{Coul} : the Coulomb interaction energy; U_{rxnf} : SGB—solvent reaction field energy; U_{cav} : the cavity energy; U_{ele} : the electrostatic energy terms in the SGB continuum solvent model, where $U_{\text{ele}} = U_{\text{Coul}} + 2U_{\text{rxnf}}$; G_{complex} : the total energy of the complex; G_{protein} : the energy of the receptor without the ligand; G_{ligand} : the energy of the unbound ligand; ΔG_{bind} : the agonist—receptor binding free energies; ΔG_{Coul} : the columbic binding free energy; ΔG_{Cov} : the covalent binding free energy; ΔG_{vdW} : the van der Waals binding free energy; $\Delta G_{\text{Solv SA}}$: the surface area solvation binding free energy; $\Delta G_{\text{Solv GB}}$: the generalized Born solvation binding free energy.

^c Correlation with two outliers (AJ9677 and CL316243).

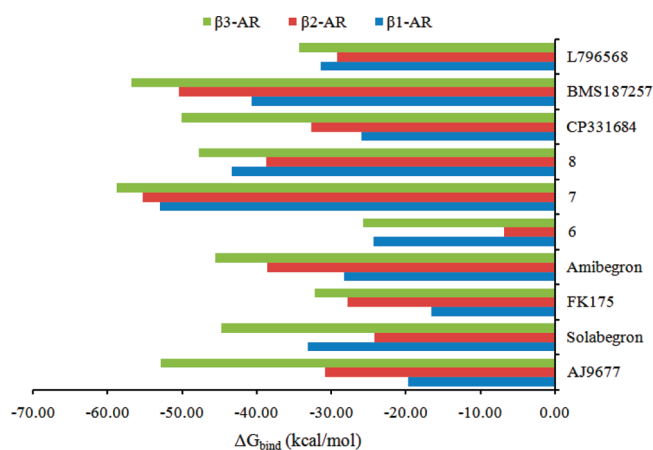


Figure 11. A graphical plot of the comparative binding free energies of the β -AR agonists into the binding site of β_1 -, β_2 -, and β_3 -ARs.

complexes. This study suggests that the ΔG_{Coul} , the net Coulomb (electrostatic) binding free energy, is the best correlate of the observed pEC_{50} of different β_3 -selective agonists with correlation coefficient (R) of 0.663 ($N = 10$), explaining about 44% of the β_3 -agonistic activity variations among 10 β_3 -selective agonists. This suggests that the long-range electrostatic (Coulomb) interaction as one of the main forces working between the agonist and receptor surface. The other Prime MM-GBSA parameters with moderate correlation coefficient (R) with the observed pEC_{50} of different β_3 -selective agonists are ΔG_{bind} ($R = 0.721$; $N = 8$) on excluding two compounds AJ9677 and CL316243 and $\Delta G_{\text{Solv GB}}$ ($R = 0.608$; $N = 10$). Among the Liaison descriptors, the two best correlations are

observed with U_{ele} ($R = 0.676$; $N = 10$) and U_{rxnf} ($R = 0.656$; $N = 10$), while other parameters, such as U_{Coul} , gave a subtle correlation coefficient of 0.365 only with the β_3 -agonistic pEC_{50} . The observed correlations of the calculated binding free energies and its components with the β_3 -agonistic pEC_{50} are moderate but acceptably good. The observed moderate correlation may be attributed to the fact that the reported β_3 -agonistic activities (pEC_{50}) for the representative β -agonists are from different research laboratories. Despite of this heterogeneity, the Liaison descriptors and Prime MM-GBSA binding free energies have outperformed the standard-precision (SP) and extra-precision (XP) glidescores toward explaining the β -agonist activity variations of the representative β -agonists. Our observation of the better performance of the Liaison descriptors and the Prime MM-GBSA end point free energies over the glidescores is consistent with the previous analyses⁶¹ reported by various researchers applied on other therapeutic class of molecules.

CONCLUSIONS

Comparative modeling of β_3 -AR based on the high-resolution crystal structure of β_2 -AR-carazolol binary complex (PDB ID: 2rh1) has resulted in a plausible homology model with highly symmetrical backbone conformations, acceptable stereochemical parameters, and side-chain packing densities. Based on the multiple sequence alignment, the decreasing order of conservation among the 7 TMs of the three subtypes of β -AR is: TM3 > TM6 > TM2 > TM7 > TM5 > TM1 > TM4. Comparison of the constructed β_3 -AR model with the crystal structure of other two subtypes (β_1 - and β_2) suggests that despite of high sequence identity and similarity in their seven TM regions, they differ in their overall helical arrangements in their extracellular (ECL1–3) and intracellular loops (ICL1–3). Inspection of the extracellular

half of the seven TMs of β -receptor subtypes, forming the solvent exposed binding site for both agonists and antagonists has highlighted few notable differences including the presence of 325^{7,32}-GPAF-328^{7,35}, 305^{7,32}-KEVY-308^{7,35}, and 323^{7,32}-DWLF-326^{7,35} sequences and R315^{6,58}, H296^{6,58}, and N313^{6,58} residues in β_3 , β_2 , and β_1 -ARs, respectively. The binding modes of 12 representative β_3 -selective agonists into the active site of β_3 -AR have revealed the energetically favored and nearly common interactions between β -hydroxyl, protonated amine, D117^{3,32}, and N332^{7,39} among all agonists and the classical small molecule transmitter (epinephrine). The only difference has been in the tightness of binding (geometric distances) of agonists with these residues D117^{3,32} and N332^{7,39} conserved in all β -receptor subtypes. Moreover, an additional three point H-bond interactions between Y336^{7,43}, the protonated amine, and β -hydroxyl group has been observed in all the representative β_3 -selective agonists, being absent in case of epinephrine and norepinephrine. This critical observation is substantiated by the very recent publication on the nanobody-stabilized active state structure of β_2 -AR bound to the full agonist, where the involvement of Y316^{7,43} is reported to interact with the protonated amine of the full agonist. The substituted aromatic groups of both the agonist and antagonist, attached to the β -hydroxyl carbon directly or through a small linker, are stabilized by the strong array of hydrophobic interactions with the localized aromatic and non-aromatic residues, namely W305^{6,48}, F308^{6,51}, F309^{6,52}, V118^{3,33}, and V121^{3,33} in the deep binding pocket accommodating the corresponding catechol ring of the epinephrine and norepinephrine. Such strong hydrophobic interactions in turn facilitate the direct salt-bridge formation of the protonated amine and the β -hydroxyl groups with the conserved residues, namely D117^{3,32} and N332^{7,39}. These hydrophobic residues W305^{6,48}, F308^{6,51}, F309^{6,52}, V118^{3,33}, and V121^{3,33}, along with the two ionizable residues D117^{3,32} and N332^{7,39}, provide a three point positional constraint, which dramatically limits the degree of conformational and rotational freedom of the bound agonists and antagonist in the binding pocket of β_3 -AR. In addition, Y336^{7,43} serves as hook for better fitting in the deep binding pocket formed by TM3 and TM5–TM7 of the β_3 -AR.

All the computational results demonstrate that the β_3 -selectivity of the representative agonists is strongly dependent on the nonconserved residues R315^{6,58} of β_3 -AR, with which carboxylate group, present in most of the representative agonists, has formed charge-enforced mono/bidentate H-bonds. This β_3 -specific residue R315^{6,58} dramatically differs from the corresponding N313^{6,58} and H296^{6,58} residues in β_1 and β_2 , respectively, in terms of its overall size, charge density, protonation potential, and overall capability to form direct H-bond and long-range electrostatic interactions with the localized residues or the acidic groups of the bound ligands. Additionally, the presence of Y308^{7,35} in β_2 -AR, in place of F325^{7,35} and F328^{7,35} in β_1 - and $\beta\beta_3$ -ARs, respectively, has been found to be one of the critical β_2 -specific residue that limits the exposure of the negatively ionizable carboxylate center of the β_3 -selective agonists to interact with the H296^{6,58} of the β_2 -AR due to relatively greater steric perturbations with the hydroxyl group of Y308^{7,35} and thus explains better agonistic activity of these representative agonists toward β_3 - and β_1 - over β_2 -ARs. Furthermore, the linker connecting the negative ionizable center to the protonated amine group has appreciable impact on the subtype selectivity as observed from the binding modes of different agonists. The distance measurements between the protonated amine and the

negative ionizable centers in the bioactive conformations of each β_3 -selective agonist bound to β_3 -AR revealed that the most optimal distance should be in the range of 9–10 Å. The residues, namely F328^{7,35} and L329^{7,36}, and the ECL2-specific F198 residues of β_3 -AR serve as respective upper and bottom supports for the aromatic part of the linker, umpiring the interaction of negatively charged center of the ligands with the β_3 -specific R315^{6,58} residue for governing subtype-selectivity. Additionally, β_3 residue A197 in the ECL2 domain, positioned adjacent to the disulfide bond of the β_3 -AR, is aspartate in both β_1 - (D200) and β_2 - (D192) receptors. The proximity of this acidic residue, combined with the lack of a compelling protonated basic partner (in β_1 - and β_2 -ARs) for the carboxylate group present in β_3 -selective ligands and the nonconserved residues in the terminal portion of TM7 near ECL2 domain, suggests a possible basis for the lower affinity of these agonists for β_1 - and β_2 - versus β_3 -receptors.

Among the computed Liaison descriptors, Prime MM-GBSA binding free energies, and its components, the reasonably good correlations of the ΔG_{Coul} , U_{ele} , and U_{rxnf} with the β_3 -agonistic activity (pEC_{50}) of the representative β -agonists have suggested the particular role of the long-range electrostatic (Coulomb) and the solvent exposed binding site interactions as the major forces present between β_3 -AR and bound agonists. The fundamental insights obtained in the present computational study are expected to be valuable for future rational design of the subtype-selective agonists targeted to specific β -AR subtypes.

■ EXPERIMENTAL SECTION

Protein Sequences and Templates Used. All sequences were retrieved from the Swiss-Prot database. The Swiss-Prot primary accession number (PAN) of β_3 -AR is P13945. The inverse-agonist bound GPCR crystal structure of human β_2 -AR (2rh1, chain A, 2.4 Å resolution)¹² was taken into account as template for homology modeling of the human β_3 -AR.

Sequence Alignment and Model Building. The multiple sequence alignment of the three subtypes of β -ARs was done initially using the ClustalW²¹ program using Blosum68 weight matrix and adjusted manually especially in TM regions. The homology modeling was done using the Modeller9v7²⁰ package based on the high resolution crystal structure of human β_2 -AR (PDB ID: 2rh1)¹² determined at 2.4 Å resolution. The default fast optimization phase given in the automatic modeling python script was modified to slow optimization (using 300 as total number of iterations) to get more plausible models. The rest settings were kept at default.

Model Quality Assessments (MQA). Currently, there is not a single method able to consistently and accurately predict the 3D structure of a protein. Similarly, there is no single method able to consistently and accurately predict the errors in a protein structure. For that reason, use of as many as possible different quality assessment (QA) methods may help in selecting the most plausible model. Different methods use different approaches, thus they can complement to each other. These QA methods are Procheck,²³ ProQ,²⁴ and ProSA-web.²⁵ These methods have been used for the quality assessment and the relevant model selection in the present study. The Procheck is employed for geometric evaluations, whereas ProsaWeb is used to evaluate the quality of consistency between the native fold and the sequence and to examine the energy of residue–residue interactions.

Ligand and Protein Preparation. Proteins were prepared using Protein Preparation Wizard implemented in Schrödinger package. The 2D structures of ligands were sketched in ISIS Draw (version 11.0) and then subsequently converted into 3D representations in the Maestro (version 9.0). The ionizable centers, such as amine, carboxylic acid, and sulfonamide, present in the ligands were ionized using the Epik mode in the LigPrep protocol of Maestro (version 9.0). An extensive conformational searching for each ligand was performed using MacroModel⁶² to ensure that concluding results were not biased by selection of only one or two low-energy conformers. The automated rigid ligand-docking exercises were performed for all low-energy conformers for each ligand into the active site of β -ARs as well as for binding affinities studies.

Molecular Docking and Scoring. The molecular docking of reported ligands into the active site of three subtypes of β -ARs was accomplished using Glide⁵² module implemented in Schrödinger software package.⁵³ The receptor grid was generated using a cocrystallized ligand in case of β_1 and β_2 -ARs, while active site residues namely, D117^{3,32}, N332^{7,39}, W305^{6,48}, S208^{5,43}, and S211^{5,46} were used for receptor grid generation in the case of modeled β_3 -AR. To relax the initial docked complexes, 100 steps of steepest-descent minimization was performed followed by low-temperature backbone-constrained molecular dynamics simulations using MacroModel module for 10 ps of heating to 30 K, 10 ps of equilibrium, and 1200 ps of production time to identify stable receptor–ligand interactions. To allow residues to be readily compared between adrenergic receptor subtypes, the standardized numbering system of Balsteros and Weinstein⁶³ is used throughout this study to identify residues in the TM helices. Along with numbering their positions in the primary amino acid sequence, the residues have numbers in parentheses (X.YZ) that indicate their position in each TM helix (X), relative to a conserved reference residue in that TM helix (YZ). However, the numbering was not used in the extra/intracellular loop regions. The key interactions between these agonists and the binding site residues of β_3 -AR are presented in the 2D form using LigandScout⁶⁴ software, while the 3D molecular graphics were produced using PyMol⁶⁵ program.

Binding Free Energy Calculations and Structure-Based Descriptor Generations. The receptor–ligand binding free energies (ΔG_{bind}) were calculated using Prime MM-GBSA⁵⁵ module implemented in Schrödinger⁵³ package considering the complexes of agonists with modeled β_3 -AR. Liaison⁶⁰ was also used to calculate structure-based descriptors by running molecular mechanics (MM) simulations of the agonist–receptor complex and of the free ligand and free receptor, with the surface generalized Born (SGB) continuum solvation model.

■ ASSOCIATED CONTENT

§ Supporting Information. Quality assessment results, distance measurements, and docked poses of representative agonists into the biding site of β_1 - and β_2 -ARs. This material is available free of charge via the Internet at <http://pubs.acs.org>.

■ AUTHOR INFORMATION

Corresponding Author

*E-mail: anilsak@gmail.com. Telephone: (522) 2612412, ext 4386.

■ ACKNOWLEDGMENT

The author (K.K.R.) is thankful to the Council of Scientific and Industrial Research for the financial assistance in the form of a fellowship. The technical assistance of Mr. A. S. Kushwaha is also acknowledged.

■ ADDITIONAL NOTE

The CDRI communication number allotted to this manuscript is 8058.

■ REFERENCES

- (1) Barness, L. A.; Opitz, J. M.; Gilbert-Barness, E. Obesity: Genetic, Molecular, and Environmental Aspects. *Am. J. Med. Genet.* **2007**, 143A, 3016–3034.
- (2) (a) Arch, J. R. S.; Ainsworth, A. T.; Cawthorne, M. A.; Piercy, V.; Sennitt, M. V.; Thody, V. E.; Wilson, C.; Wilson, S. Atypical β -Adrenoceptor on Brown Adipocytes as Target for Anti-Obesity Drugs. *Nature* **1984**, 309, 163–165. (b) Hu, B.; Jennings, L. L. Orally Bioavailable β_3 -Adrenergic Receptor Agonists as Potential Therapeutic Agents for Obesity and Type-II Diabetes. *Prog. Med. Chem.* **2003**, 41, 167–194.
- (3) Shakya, N.; Roy, K. K.; Saxena, A. K. Substituted 1,2,3,4-Tetrahydroquinolin-6-yloxypropanes as β_3 -Adrenergic Receptor Agonists: Design, Synthesis, Biological Evaluation and Pharmacophore Modeling. *Bioorg. Med. Chem.* **2009**, 17, 830–847.
- (4) Ursino, M. G.; Vasinaa, V.; Raschia, E.; Cremab, F.; Pontia, F. D. The β_3 -Adrenoceptor as a Therapeutic Target: Current Perspectives. *Pharmacol. Res.* **2009**, 59, 221–234.
- (5) Rosenbaum, D. M.; Rasmussen, S. G.; Kobilka, B. K. The Structure and Function of G-Protein-Coupled Receptors. *Nature* **2009**, 459, 356–363.
- (6) Bissantz, C.; Bernard, P.; Hibert, M.; Rognan, D. Protein-Based Virtual Screening of Chemical Databases. II. Are Homology Models of G-Protein Coupled Receptors Suitable Targets? *Proteins: Struct., Funct., Genet.* **2003**, 50, 5–25.
- (7) Archer, E.; Maigret, B.; Escrieut, C.; Pradayrol, L.; Fourmy, D. Rhodopsin Crystal: New Template Yielding Realistic Models of G-Protein-Coupled Receptors? *Trends Pharmacol. Sci.* **2003**, 24, 36–40.
- (8) Chambers, J. J.; Nichols, D. E. A Homology-Based Model of the Human 5-HT_{2A} Receptor Derived from an *In Silico* Activated G-Protein Coupled Receptor. *J. Comput.-Aided Mol. Des.* **2002**, 16, 511–520.
- (9) Ding, X.-Q.; Pinon, D. I.; Furse, K. E.; Lybrand, T. P.; Miller, L. J. Refinement of the Conformation of a Critical Region of Charge-Charge Interaction between Cholecystokinin and its Receptor. *Mol. Pharmacol.* **2002**, 61, 1041–1052.
- (10) Costanzi, S. On the Applicability of GPCR Homology Models to Computer-Aided Drug Discovery: a Comparison Between *In Silico* and Crystal Structures of the β_2 -Adrenergic Receptor. *J. Med. Chem.* **2008**, 51, 2907–2914.
- (11) Furse, K. E.; Lybrand, T. P. Three-Dimensional Models for β -Adrenergic Receptor Complexes with Agonists and Antagonists. *J. Med. Chem.* **2003**, 46, 4450–4462.
- (12) Cherezov, V.; Rosenbaum, D. M.; Hanson, M. A.; Rasmussen, S. G. F.; Thian, F. S.; Kobilka, T. S.; Choi, H. -J.; Kuhn, P.; Weis, W. I.; Kobilka, B. K.; Stevens, R. C. High-Resolution Crystal Structure of an Engineered Human β_2 -Adrenergic G-Protein Coupled Receptor. *Science* **2007**, 318, 1258–1265.
- (13) Rasmussen, S. G.; Choi, H. J.; Fung, J. J.; Pardon, E.; Casarosa, P.; Chae, P. S.; Devree, B. T.; Rosenbaum, D. M.; Thian, F. S.; Kobilka, T. S.; Schnapp, A.; Konetzki, I.; Sunahara, R. K.; Gellman, S. H.; Pautsch, A.; Steyaert, J.; Weis, W. I.; Kobilka, B. K. Structure of a Nanobody-Stabilized Active State of the β_2 -Adrenoceptor. *Nature* **2011**, 469, 175–180.
- (14) Guan, X. M.; Amend, A.; Strader, C. D. Determination of Structural Domains for G-Protein Coupling and Ligand Binding in β_3 -Adrenergic Receptor. *Mol. Pharmacol.* **1995**, 48, 492–498.

- (15) Piétri-Rouxel, F.; St John Manning, B.; Gros, J.; Strosberg, A. D. The Biochemical Effect of the Naturally Occurring Trp64-Arg Mutation on Human β_3 -Adrenoceptor Activity. *Eur. J. Biochem.* **1997**, *247*, 1174–1179.
- (16) Gros, J.; Manning, B. S.; Pietri-Rouxel, F.; Guillaume, J. L.; Drumare, M. F.; Strosberg, A. D. Site-Directed Mutagenesis of the Human β_3 -Adrenoceptor: Transmembrane Residues Involved in Ligand Binding and Signal Transduction. *Eur. J. Biochem.* **1998**, *251*, 590–596.
- (17) Granneman, J. G.; Lahners, K. N.; Zhai, Y. Agonist Interactions with Chimeric and Mutant β_1 - and β_3 -Adrenergic Receptors: Involvement of the Seventh Transmembrane Region in Conferring Subtype Specificity. *Mol. Pharmacol.* **1998**, *53*, 856–861.
- (18) Forrest, L. R.; Tang, C. L.; Honig, B. On the Accuracy of Homology Modeling and Sequence Alignment Methods Applied to Membrane Proteins. *Biophys. J.* **2006**, *91*, 508–517.
- (19) Mobarec, J. C.; Sanchez, R.; Filizola, M. Modern Homology Modeling of G-Protein Coupled Receptors: Which Structural Template to Use? *J. Med. Chem.* **2009**, *52*, 5207–5216.
- (20) Eswar, N.; Marti-Renom, M. A.; Webb, B.; Madhusudhan, M. S.; Eramian, D.; Shen, M.; Pieper, U.; Sali, A. *Current Protocols in Bioinformatics*; John Wiley & Sons, Inc.: Totowa, New Jersey, 2006; Supplement 15, 5.6.1–5.6.30.
- (21) Thompson, J. D.; Higgins, D. G.; Gibson, T. J.; CLUSTAL W Improving the Sensitivity of Progressive Multiple Sequence Alignment through Sequence Weighting, Position Specific Gap Penalties and Weight Matrix Choice. *Nucleic Acids Res.* **1994**, *22*, 4673–4680.
- (22) (a) Ghanouni, P.; Steenhuis, J. J.; Farrens, D. L.; Kobilka, B. K. Agonist-Induced Conformational Changes in the G-Protein-Coupling Domain of the β_2 -Adrenergic Receptor. *Proc. Natl. Acad. Sci. U.S.A.* **2001**, *98*, 5997–6002. (b) Dohlman, H. G.; Caron, M. G.; Strader, C. D.; Amalaiky, N.; Lefkowitz, R. J. Identification and Sequence of a Binding Site Peptide of the β_2 -Adrenergic Receptor. *Biochemistry* **1988**, *27*, 1813–1817. (c) Savarese, T. M.; Fraser, C. M. In Vitro Mutagenesis and Search for Structure-Function Relationships among G-Protein Coupled Receptors. *Biochem. J.* **1992**, *283*, 1–19. (d) Strader, C. D.; Fong, T. M.; Tota, M. R.; Underwood, D.; Dixon, R. A. F. Structure and Function of G-Protein Coupled Receptors. *Annu. Rev. Biochem.* **1994**, *63*, 101–132.
- (e) Hockerman, G. H.; Girvin, M. E.; Malbon, C. C.; Ruoho, A. E. Antagonist Conformations with the β_2 -Adrenergic Receptor Ligand Binding Pocket. *Mol. Pharmacol.* **1996**, *49*, 1021–1032. (f) Isogaya, M.; Sugimoto, Y.; Tanimura, R.; Tanaka, R.; Kikkawa, H.; Nagao, T.; Kurose, H. Binding Pockets of the β_1 - and β_2 -Adrenergic Receptors for Subtype-Selective Agonists. *Mol. Pharmacol.* **1999**, *56*, 875–885. (g) Wong, S. K. –F.; Slaughter, C.; Ruoho, A. E.; Ross, E. M. The Catecholamine Binding Site of the β -Adrenergic Receptor is formed by Juxtaposed Membrane-Spanning Domains. *J. Biol. Chem.* **1988**, *263*, 7925–7928.
- (23) Laskowski, R. A.; MacArthur, M. W.; Moss, D. S.; Thornton, J. M.; PROCHECK, A Program to Check the Stereochemical Quality of Protein Structures. *J. Appl. Crystallogr.* **1993**, *26*, 283–291.
- (24) Wallner, B.; Elofsson, A. Can Correct Protein Models be Identified? *Protein Sci.* **2003**, *12*, 1073–1086.
- (25) Wiederstein, M.; Sippl, M. J. ProSA-web: Interactive Web Service for the Recognition of Errors in Three-Dimensional Structures of Proteins. *Nucleic Acids Res.* **2007**, *35*, W407–W410.
- (26) Sansom, M. S. P.; Weinstein, H. Hinges, Swivels, and Switches: The Role of Prolines in Signaling via Transmembrane Alpha-Helices. *Trends Pharmacol. Sci.* **2000**, *21*, 445–451.
- (27) Okada, T.; Sugihara, M.; Bondar, A. N.; Elstner, M.; Entel, P.; Buss, V. The Retinal Conformation and its Environment in the Light of New 2.2 Å Crystal Structure. *J. Mol. Biol.* **2004**, *342*, 571–581.
- (28) Palczewski, K.; Kumakura, T.; Hori, T.; Behnke, C. A.; Motoshima, H.; Fox, B. A.; Le –Trong, I.; Teller, D. C.; Okada, T.; Stenkamp, R. E.; Yamamoto, M.; Miyano, M. Crystal Structure of Rhodopsin: A G-Protein Coupled Receptor. *Science* **2000**, *289*, 739–J745.
- (29) Vogel, R.; Mahalingam, M.; Lüdeke, S.; Huber, T.; Siebert, F.; Sakmar, T. P. Functional Role of the “Ionic Lock”- an Interhelical Hydrogen-Bond Network in Family-A Heptahelical Receptors. *J. Mol. Biol.* **2008**, *380*, 648–655.
- (30) Ballesteros, J. A.; Jensen, A. D.; Liapakis, G.; Rasmussen, S. G.; Shi, L.; Gether, U.; Javitch, J. A. Activation of the β_2 -Adrenergic Receptor Involves Disruption of an Ionic Lock Between the Cytoplasmic Ends of Transmembrane Segments 3 and 6. *J. Biol. Chem.* **2001**, *276*, 29171–29177.
- (31) Hanson, M. A.; Stevens, R. C. Discovery of New GPCR Biology: One Receptor Structure at a Time. *Structure* **2009**, *17*, 8–14.
- (32) Hanson, M. A.; Cherezov, V.; Roth, C. B.; Griffith, M. T.; Jaakola, V. –P.; Chien, E. Y. T.; Velasquez, J.; Kuhn, P.; Stevens, R. C. A Specific Cholesterol Binding Site is Established by the 2.8 Å Structure of the Human β_2 -Adrenergic Receptor. *Structure* **2008**, *16*, 897–905.
- (33) Jaakola, V. P.; Griffith, M. T.; Hanson, M. A.; Cherezov, V.; Chien, E. Y.; Lane, J. R.; Ijzerman, A. P.; Stevens, R. C. The 2.6 Å Crystal Structure of a Human A_{2A} Adenosine Receptor Bound to an Antagonist. *Science* **2008**, *322*, 1211–1217.
- (34) Warne, T.; Serrano-Vega, M. J.; Baker, J. G.; Moukhametzianov, R.; Edwards, P. C.; Henderson, R.; Leslie, A. G.; Tate, C. G.; Schertler, G. F. Structure of a β_1 -Adrenergic G-Protein Coupled Receptor. *Nature* **2008**, *454*, 486–491.
- (35) Chien, E. Y. T.; Liu, W.; Zhao, Q.; Katritch, V.; Han, G. W.; Hanson, M. A.; Shi, L.; Newman, A. H.; Javitch, J. A.; Cherezov, V.; Stevens, R. C. Structure of the Human Dopamine D₃ Receptor in Complex with a D₂/D₃ Selective Antagonist. *Science* **2010**, *330*, 1091–1095.
- (36) Rosenbaum, D. M.; Rasmussen, S. G. F.; Kobilka, B. K. The Structure and Function of G-Protein Coupled Receptors. *Nature* **2009**, *459*, 356–363.
- (37) Liapakis, G.; Ballesteros, J. A.; Papachristou, S.; Chan, W. C.; Chen, X.; Javitch, J. A. The Forgotten Serine: A Critical Role for Ser-203^{S^{A2}} in Ligand Binding to and Activation of the β_2 -Adrenergic Receptor. *J. Biol. Chem.* **2000**, *275*, 37779–37788.
- (38) Kikkawa, H.; Isogaya, M.; Nagao, T.; Kurose, H. The Role of the Seventh Transmembrane Region in High Affinity Binding of a β_2 -Selective Agonist TA-2005. *Mol. Pharmacol.* **1998**, *53*, 128–134.
- (39) Harada, H.; Hirokawa, Y.; Suzuki, K.; Hiyama, Y.; Oue, M.; Kawashima, H.; Yoshida, N.; Furutani, Y.; Kato, S. Novel and Potent Human and Rat β_3 -Adrenergic Receptor Agonists Containing Substituted 3-Indolylalkylamines. *Bioorg. Med. Chem. Lett.* **2003**, *13*, 1301–1305.
- (40) Uehling, D. E.; Shearer, B. G.; Donaldson, K. H.; Chao, E. Y.; Deaton, D. N.; Adkison, K. K.; Brown, K. K.; Cariello, N. F.; Faison, W. L.; Lancaster, M. E.; Lin, J.; Hart, R.; Milliken, T. O.; Paulik, M. A.; Sherman, B. W.; Sugg, E. E.; Cowan, C. Biaryliline Phenethanolamines as Potent and Selective β_3 -Adrenergic Receptor Agonists. *J. Med. Chem.* **2006**, *49*, 2758–2771.
- (41) Imanishi, M.; Nakajima, Y.; Tomishima, Y.; Hamashima, H.; Washizuka, K.; Sakurai, M.; Matsui, S.; Imamura, E.; Ueshima, K.; Yamamoto, T.; Yamamoto, N.; Ishikawa, H.; Nakano, K.; Unami, N.; Hamada, K.; Matsumura, Y.; Takamura, F.; Hattori, K. Discovery of a Novel Series of Benzoic Acid Derivatives as Potent and Selective Human β_3 -Adrenergic Receptor Agonists with Good Oral Bioavailability. 3. Phenylethanolaminotetraline (PEAT) Skeleton Containing Biphenyl or Biphenyl Ether Moiety. *J. Med. Chem.* **2008**, *51*, 4804–4822.
- (42) Bloom, J. D.; Dutia, M. D.; Johnson, B. D.; Wissner, A.; Burns, M. G.; Largis, E. E.; Dolan, J. A.; Claus, T. H. Disodium (R,R)-5-[2-[2-(3-chlorophenyl)-2-hydroxyethyl]-amino]propyl]-1,3-benzodioxole-2,2-dicarboxylate (CL-316,243). A Potent β -Adrenergic Agonist Virtually Specific for β_3 -Receptors. A Promising Antidiabetic and Antiobesity agent. *J. Med. Chem.* **1992**, *35*, 3081–3084.
- (43) Shearer, B. G.; Chao, E. Y.; Uehling, D. E.; Deaton, D. N.; Cowan, C.; Sherman, B. W.; Milliken, T.; Faison, W.; Brown, K.; Adkison, K. K.; Lee, F. Synthesis and Evaluation of Potent and Selective β_3 -Adrenergic Receptor Agonists Containing Heterobiaryl Carboxylic Acids. *Bioorg. Med. Chem. Lett.* **2007**, *17*, 4670–4677.
- (44) Finley, D. R.; Bell, M. G.; Borel, A. G.; Bloomquist, W. E.; Cohen, M. L.; Heiman, M. L.; Kriauciunas, A.; Matthews, D. P.; Miles,

- T.; Neel, D. A.; Rito, C. J.; Sall, D. J.; Shuker, A. J.; Stephens, T. W.; Tinsley, F. C.; Winter, M. A.; Jesudason, C. D. Potent Benzimidazolone Based Human β_3 -Adrenergic Receptor Agonists. *Bioorg. Med. Chem. Lett.* **2006**, *16*, 5691–5694.
- (45) Sum, F. W.; Wong, V.; Han, S.; Largis, E.; Mulvey, R.; Tillett, J. Cyclic Amine Sulfonamides as Linkers in the Design and Synthesis of Novel Human β_3 -Adrenergic Receptor Agonists. *Bioorg. Med. Chem. Lett.* **2003**, *13*, 2191–2194.
- (46) Uchida, H.; Shishido, K.; Nomiya, M.; Yamaguchi, O. Involvement of Cyclic AMP-Dependent and -Independent Mechanisms in the Relaxation of Rat Detrusor Muscle via β -Adrenoceptors. *Eur. J. Pharmacol.* **2005**, *518*, 195–202.
- (47) Tomiyama, Y.; Murakami, M.; Hayakawa, K.; Akiyama, K.; Yamazaki, Y.; Kojima, M.; Shibata, N.; Akahane, M. Pharmacological Profile of KUL-7211, a Selective β_3 -Adrenoceptor Agonist, in Isolated Ureteral Smooth Muscle. *J. Pharmacol. Sci.* **2003**, *92*, 411–419.
- (48) Tanaka, N.; Tamai, T.; Mukaiyama, H.; Hirabayashi, A.; Muranaka, H.; Ishikawa, T.; Kobayashi, J.; Akahane, S.; Akahane, M. Relationship between Stereochemistry and the β_3 -Adrenoceptor Agonistic Activity of 4'-Hydroxynorephedrine Derivative as an Agent for Treatment of Frequent Urination and Urinary Incontinence. *J. Med. Chem.* **2003**, *46*, 105–112.
- (49) Fisher, L. G.; Sher, P. M.; Skwisch, S.; Michel, I. M.; Seiler, S. M.; Dickinson, K. E. J. BMS-187257, a Potent, Selective, And Novel Heterocyclic β_3 -Adrenergic Receptor Agonist. *Bioorg. Med. Chem. Lett.* **1996**, *6*, 2253–2258.
- (50) (a) van Baak, M. A.; Hul, G. B.; Toubo, S.; Astrup, A.; Gottesdiener, K. M.; DeSmet, M.; Saris, W. H. Acute Effect of L-796568, a Novel β_3 -Adrenergic Receptor Agonist, on Energy Expenditure in Obese Men. *Clin. Pharmacol. Ther.* **2002**, *71*, 272–279. (b) Mathvink, R. J.; Tolman, J. S.; Chitty, D.; Candelore, M. R.; Cascieri, M. A.; Colwell, L. F., Jr.; Deng, L.; Feeney, W. P.; Forrest, M. J.; Hom, G. J.; MacIntyre, D. E.; Miller, R. R.; Stearns, R. A.; Tota, L.; Wyvratt, M. J.; Fisher, M. H.; Weber, A. E. Discovery of a Potent, Orally Bioavailable β_3 -Adrenergic Receptor Agonist, (R)-N-[4-[2-[(2-Hydroxy-2-(3-pyridinyl)ethyl]amino]ethyl]phenyl]-4-[4-[4-(trifluoromethyl)phenyl]thiazol-2-yl]benzenesulfonamide. *J. Med. Chem.* **2000**, *43*, 3832–3836.
- (51) Nisoli, E.; Tonello, C.; Landi, M.; Carruba, M. O. Functional Studies of the First Selective β_3 -Adrenergic Receptor Antagonist SR 59230A in Rat Brown Adipocytes. *Mol. Pharmacol.* **1996**, *49*, 7–14.
- (52) Glide, version 5.0; Schrödinger: LLC: New York, 2008.
- (53) Schrödinger, version 8.0; Schrödinger, LLC: New York, 2005.
- (54) (a) Strader, C. D.; Sigal, I. S.; Candelore, M. R.; Hill, W. S.; Dixon, R. A. F. Conserved Aspartic Acid Residues 79 and 113 of the β -Adrenergic Receptor have Different Roles in Receptor Function. *J. Biol. Chem.* **1988**, *263*, 10267–10271. (b) Strader, C. D.; Candelore, M. R.; Hill, W. S.; Sigal, I. S.; Dixon, R. A. F. Identification of Two Serine Residues Involved in Agonist Activation of the β -Adrenergic Receptor. *J. Biol. Chem.* **1989**, *264*, 13572–13578.
- (55) Wieland, K.; Zuurmond, H. M.; Krasel, C.; Ijzerman, A. P.; Lohse, M. J. Involvement of Asn-293 in Stereospecific Agonist Recognition and in Activation of the β_2 -Adrenergic Receptor. *Proc. Natl. Acad. Sci. U.S.A.* **1996**, *93*, 9276–9281.
- (56) Suryanarayana, S.; Kobilka, B. K. Amino Acid Substitutions at Position 312 in the Seventh Hydrophobic Segment of the β_2 -Adrenergic Receptor Modify Ligand-Binding Specificity. *Mol. Pharmacol.* **1993**, *44*, 111–114.
- (57) Kuipers, W.; Link, R.; Standaar, P. J.; Stoit, A. R.; van Wijngaarden, I.; Leurs, R.; Ijzerman, A. P. Study of the Interaction Between Aryloxypropanolamines and Asn-386 in Helix VII of the Human 5-Hydroxytryptamine-1A Receptor. *Mol. Pharmacol.* **1997**, *51*, 889–896.
- (58) Frielle, T.; Daniel, K. W.; Caron, M. G.; Lefkowitz, R. J. Structural Basis of β -Adrenergic Receptor Subtype Specificity Studied with Chimeric β_1/β_2 -Adrenergic Receptors. *Proc. Natl. Acad. Sci. U.S.A.* **1988**, *85*, 9494–9498.
- (59) Prime, version 2.1; Schrödinger, LLC: New York, 2005.
- (60) Liaison, version 5.5; Schrödinger, LLC: New York, 2009.
- (61) (a) Jorgensen, W. L. Free Energy Calculations: A Breakthrough for Modeling Organic Chemistry in Solution. *Acc. Chem. Res.* **1989**, *22*, 184–189. (b) Kollman, P. A. Free Energy Calculations: Applications to Chemical and Biochemical Phenomena. *Chem. Rev.* **1993**, *93*, 2395–2417. (c) Simonson, T.; Georgios, A.; Karplus, M. Free Energy Simulations Come of Age: Protein-Ligand Recognition. *Acc. Chem. Res.* **2002**, *35*, 430–437. (d) Pearlman, D. A.; Charifson, P. S. Are Free Energy Calculations Useful in Practice? A Comparison with Rapid Scoring Functions for the p38 MAP Kinase Protein System. *J. Med. Chem.* **2001**, *44*, 3417–3423. (e) Guimaraes, C. R. W.; Boger, D. L.; Jorgensen, W. L. Elucidation of Fatty Acid Amide Hydrolase Inhibition by Potent R-Keto-heterocycle Derivatives from Monte Carlo Simulations. *J. Am. Chem. Soc.* **2005**, *127*, 17377–17384. (f) Lee, M. R.; Sun, Y. Improving Docking Accuracy Through Molecular Mechanics Generalized Born Optimization and Scoring. *J. Chem. Theory Comput.* **2007**, *3*, 1106–1119.
- (62) MacroModel, version 9.8; Schrödinger, LLC: New York, 2010.
- (63) Ballesteros, J. A.; Weinstein, H. Integrated Methods for the Construction of Three Dimensional Models and Computational Probing of Structure Function Relations in G-Protein Coupled Receptors. *Methods Neurosci.* **1995**, *25*, 366–428.
- (64) Wolber, G.; Langer, T. LigandScout: 3-D Pharmacophores Derived from Protein Bound Ligands and their Use as Virtual Screening Filters. *J. Chem. Inf. Model.* **2005**, *45*, 160–169.
- (65) The PyMOL Molecular Graphics System, version 1.3r1; Schrödinger, LLC: Portland, OR, 2010.